



**HAL**  
open science

## Palaeoenvironmental reconstructions during the Mesolithic to Neolithic transition (9.2–5.3 cal. ka BP) in Northwestern France: Palynological evidences

Clément Lambert, Muriel Vidal, Aurélie Pénaud, Pascal P. Le Roy, Evelyne Goubert, Yvan Pailler, Pierre Stéphane, Axel Ehrhold

### ► To cite this version:

Clément Lambert, Muriel Vidal, Aurélie Pénaud, Pascal P. Le Roy, Evelyne Goubert, et al.. Palaeoenvironmental reconstructions during the Mesolithic to Neolithic transition (9.2–5.3 cal. ka BP) in Northwestern France: Palynological evidences. *The Holocene*, 2019, 29 (3), pp.380-402. 10.1177/0959683618816457 . hal-02369521

**HAL Id: hal-02369521**

**<https://hal.science/hal-02369521v1>**

Submitted on 13 Apr 2021

**HAL** is a multi-disciplinary open access archive for the deposit and dissemination of scientific research documents, whether they are published or not. The documents may come from teaching and research institutions in France or abroad, or from public or private research centers.

L'archive ouverte pluridisciplinaire **HAL**, est destinée au dépôt et à la diffusion de documents scientifiques de niveau recherche, publiés ou non, émanant des établissements d'enseignement et de recherche français ou étrangers, des laboratoires publics ou privés.

---

## Palaeoenvironmental reconstructions during the Meso- to Neolithic transition (9.2–5.3 cal. ka BP) in Northwestern France: Palynological evidences

Lambert Clément<sup>1,\*</sup>, Vidal Muriel<sup>1</sup>, Penaud Aurélie<sup>1</sup>, Le Roy Pascal<sup>1</sup>, Goubert Evelyne<sup>2</sup>, Pailler Yvan<sup>3</sup>, Stephan Pierre<sup>4</sup>, Ehrhold Axel<sup>5</sup>

<sup>1</sup> Laboratoire Géosciences Océan (UMR 6538), IUEM, CNRS, Université de Bretagne Occidentale (UBO), France

<sup>2</sup> Laboratoire Géosciences Océan (UMR 6538), IUEM, CNRS, Université de Bretagne Occidentale (UBO), Université Bretagne Sud, France

<sup>3</sup> Grand-Ouest, INRAP, France

<sup>4</sup> LETG Brest GEOMER, IUEM, UMR 6554, CNRS, Université de Bretagne Occidentale (UBO), France

<sup>5</sup> Géosciences Marines, Centre de Brest, IFREMER, France

\* Corresponding author : Clément Lambert, email address : [clement.lambert24@gmail.com](mailto:clement.lambert24@gmail.com)

---

### Abstract :

Sedimentological, palynological, and micropalaeontological studies carried out throughout the first half of the Holocene, during the Mesolithic/Neolithic transition in the Bay of Brest (i.e. 9200–9000 and 6600–5300 cal. BP) and in the Bay of Douarnenez (i.e. 9200–8400 cal. BP), allowed characterizing coastal environmental changes under the increasing influence of the relative sea-level rise. The gradual flooding of the two studied sites implied a transition from river valleys to oceanic bays as revealed by the gradual retreat of salt marsh environments, as detected through palynological analysis. In addition, these high-resolution studies highlight the regional imprint of the North Atlantic millennial climate variability in north-western coastal environments. Two cold climate events are indeed suggested to have been locally marked by a moisture increase, mainly detected by increases in *Lingulodinium machaerophorum*, *Corylus*, and *Alnus* percentages at 8550 cal. BP in the Bay of Douarnenez and at 6250 cal. BP in the Bay of Brest. Moreover, regarding the Neolithic transition timing in the Bay of Douarnenez, large pollen grains of Poaceae (i.e. Cerealia-type pollen grains) have been detected at around 8600 cal. BP, that is, 1500 years before the general accepted cereal cropping appearance in Western France. These results, consistent with other palynological studies conducted in the French Atlantic coast, could underline a Mesolithic 'proto-agriculture' in Brittany.

**Keywords :** benthic foraminifera, climate variability, dinoflagellate cysts, human impacts, palaeoenvironments reconstructions, pollen grains

# 1. Introduction

The Holocene is characterized by a gradual decrease in summer air temperatures and seasonality (seasonal thermal amplitude) in line with the continuing summer insolation decrease at 65°N (*Berger and Loutre, 1991*). Sub-millennial climate variability is superimposed on this long-term climate trend, as shown by numerous studies carried out on marine (e.g. *Bond et al., 1997, 2001; Mayewski et al., 2004*), terrestrial (e.g. *Davis et al., 2003*) and glacial records (e.g. *O'Brien et al., 1995*), highlighting iterated abrupt climate events also referred as “Bond events” (*Bond et al., 1997, 2001*) or RCC (i.e. “Rapid Climate Change”; *Mayewski et al., 2004*). These events are often associated with significant climate cooling in North Atlantic surface waters and over northern Europe, as well as increasing aridity in the tropics (*Mayewski et al., 2004; Hammarlund et al., 2005; Wanner et al., 2011*). Finally, on decadal to multi-decadal timescales, climate over northern Europe is forced by the combined influences of atmospheric and oceanic natural oscillations, themselves driven by different teleconnections and physico-chemical exchanges at the air/ocean interface (*Knight et al., 2006; Tréguer et al., 2014; McCarthy et al., 2015; Ruprich-Robert and Cassou, 2015*).

The geographical exposure of the coast to the ocean and North Atlantic climate hazards thus makes the Northwest coast of France a favorite environment for the study of current and past climate. In addition to these factors, coastal areas are constantly changing shaped by different dynamic agents. The sea level-rise occurring across the deglaciation has also impacted coastal environments from a geomorphological, sedimentological and ecological point of view. On a regional scale, recent studies reconstructed and quantified the post-glacial sea-level rise on Brittany’s coasts (*Goslin et al., 2013, 2015; Stéphan et al., 2015; García-Artola et al., 2018*), estimated from about 10 to 15 mm/year between the end of the last glacial period and 9,000 years cal BP to around 4.6 mm/year between 7,500 and 6,500 years cal BP, and less than 1

69 mm/year after 6,000 years cal BP. Moreover, palaeoecological data recently acquired on  
70 Holocene Brittany's coastal sequences discussed past environmental variations (vegetation  
71 changes, palaeo-storm dynamics, precipitation regimes) and linked these rapid coastal  
72 changes with climate dynamics as well as human occupation on watersheds (*Fernane et al.,*  
73 *2014, 2015*). These studies especially focused on the Neolithic, a period when the  
74 development of agro-pastoral societies became more and more pronounced (*Visset and*  
75 *Bernard, 2006; Pailler et al., 2011*).

76 In this study, new sequences retrieved in two sites from the westernmost part of Brittany (NW  
77 France), the Bay of Brest (BB) and the Bay of Douarnenez (BD), cover the Mesolithic to  
78 Neolithic transition, a still fairly unknown period so far. They allow a multidisciplinary  
79 approach based on pollen, dinoflagellate cyst (dinocyst) and foraminiferal analyses, as well as  
80 on stable isotopes and sedimentological data. Pollen analysis provides information regarding  
81 surrounding vegetation changes on BB and BD watersheds through time. Indeed,  
82 palynological studies carried out on modern BB sediments (*Lambert et al., 2017*), as well as  
83 across the last 150 years (*Lambert et al., 2018*), evidenced the robustness of studying  
84 fossilized pollen grains in BB sediment archives to discuss both natural and anthropogenic  
85 forcings. These include: hydrodynamics, fluvial discharges, pollination rates, or agricultural  
86 watershed policy. Dinoflagellates are phytoplanktonic organisms that play an important role  
87 in the trophic network. Numerous studies carried out on modern marine sediments showed  
88 specific patterns regarding the spatial distribution of fossilizable dinocysts according to sea-  
89 surface temperature and salinity, sea-ice cover duration, inshore-offshore gradient and/or  
90 nutrient concentration (*Morzadec-Kerfourn, 1977, 1979; Dodge et Harland, 1991; Rochon et*  
91 *de Vernal, 1994; Mudie et al., 2001; Marret and Zonneveld, 2003; Zonneveld et al., 2013; de*  
92 *Vernal et al., 2013*). These palynomorphs have been observed with extremely low  
93 concentrations and a poor species richness in modern BB sediments (*Lambert et al., 2017*) but

94 have proved to be excellent markers for reconstructing past BB sea-surface conditions across  
95 the last century (*Lambert et al., 2018*). Finally, benthic foraminifera are particularly sensitive  
96 to various environmental factors (temperature, salinity, oxygenation, pH, hydrodynamism,  
97 organic matter export, water depth) and are frequently used to reconstruct bottom water-  
98 column conditions (*Goody, 2003; Jorissen et al., 2007*). In coastal environments,  
99 foraminiferal species allow reconstructing natural or human-induced environmental changes  
100 (*Debenay et al., 2006; Delaine et al., 2015*), and among the rare studies conducted in the BB  
101 with this proxy, *Stéphan (2008)* applied it to discuss palaeobathymetric evolution in salt-  
102 marsh environments related to the Holocene sea-level rise (*Stéphan and Goslin, 2014 ;*  
103 *Stéphan et al., 2015; García-Artola et al., 2018*).

104 In this paper, we thus aim at discussing the combined influences of local (i.e. watersheds)  
105 *versus* regional (i.e. northern European climate) factors driving paleoenvironmental changes  
106 across the first half of the Holocene in western Brittany (from 9,200 to 5,300 cal BP), thanks  
107 to a cross-correlated pollen-dinocyst-foraminiferal analysis and a pluri-decadal timescale  
108 resolution. Furthermore, the studied period covers the Mesolithic to the Neolithic transition,  
109 where the environmental changes thanks to the Neolithization must be detectable in  
110 paleoenvironmental sequences.

## 111 **2. Environmental contexts**

112

### 113 **2.1. Present and past sedimentological contexts of study sites**

114 The cores selected for this study are located in the westernmost part of Brittany, in marine  
115 coastal bays located on both sides of the Crozon peninsula (Fig. 1a).

116

117 **The Bay of Douarnenez (BD)**

118 The BD is a large circular bay (350 km<sup>2</sup>) limited by the Crozon peninsula to the North and the  
119 Cap Sizun to the South, largely connected to the Iroise Sea by a passage of about 9 km wide  
120 (Fig. 1b). Its bathymetry reveals a concave morphology characterized by a water depth of  
121 about 20 m, reaching 30 m in the center of the bay (Augris et al., 2005; Fig. 1b). The  
122 geological basement of the BD and its surroundings corresponds to Brioverian/Palaeozoic  
123 sandstones and schist in the North, and metamorphic/plutonic formations in the South (Mélou  
124 and Plusquellec, 1974; Augris et al., 2005). A major NW-SE trending fault network  
125 (Kerforne fault system) affects the BD, inherited from the Hercynian orogeny and reactivated  
126 during the North Atlantic opening (Lefort, 1973; Ballèvre et al., 2013). Coasts are mainly  
127 shaped by cliffs up to 100 m high in the Crozon peninsula and 85 m towards the Cap Sizun.  
128 Some valleys and small estuaries drain very restricted watersheds (40 km<sup>2</sup> for the larger),  
129 sometimes open between cliffs, protecting wetlands and marshes behind the shoreline (Augris  
130 et al., 2005). The BD does not receive a large amount of freshwater, implying a strong marine  
131 influence with a maximum tidal amplitude of 8 m and a relatively stable salinity (around  
132 35‰; Augris et al., 2005).

133 The BD sedimentary cover mainly consists of gravels and coarse sands in the central part of  
134 the bay and fine sands in sheltered areas (Hinschberger and Pauvret, 1968; Augris et al.,  
135 1988), reaching a thickness of 18 m in palaeo-valley axes, but remaining relatively thin over  
136 the whole BD (2 to 4 m; Augris et al., 2005). The substratum study reveals a dendritic palaeo-  
137 channel network incising Brioverian basement and flowing into a main valley in the center of  
138 the bay named the Ys palaeo-valley (Fig. 1b). These channels are connected to the main  
139 continental rivers surrounding the BD (Musset, 1934; Guilcher, 1948; Hallegouët, 1989;  
140 Jouet et al., 2003). The sedimentary infilling history of the BD is based on the analysis of  
141 seismic units (U1 to U6; Fig. 2) combined with analysis of numerous sediment cores (Jouet et

142 *al.*, 2003; *Le Roy and Jouet, 2005*). While the BD was totally emerged during the Last Glacial  
143 Maximum (around 20,000 years BP), its flooding, initially confined to palaeo-valleys  
144 (10,000-8,000 years BP, meander bar units U3 and U4; Fig. 2), then spread out to the rest of  
145 the BD (8,000-5,000 years BP, fine estuarine sedimentation U5; Fig. 2). The sea level was  
146 stabilized at about 6,000-5,000 years BP (*Goslin et al., 2015*) and, since then, reworked  
147 marine sands form the upper unit of the BD sediment cover (U6; Fig. 2).

148

### 149 **The Bay of Brest (BB)**

150 The BB is located in north-western Brittany (NW France; Fig. 1c) and consists of a shallow  
151 semi-enclosed basin of 180 km<sup>2</sup> surrounded by a 230 km long coastline. Its basement  
152 corresponds to Proterozoic igneous rocks in the north and Brioverian/Palaeozoic sediments in  
153 the south and east. Present-day low reliefs (few hills reach 330 m high) are inherited from the  
154 peneplanation of the Hercynian chain (*Chauris and Plusquellec, 1980; Ballèvre et al., 2009*).  
155 The study area has been subsiding since the Eocene and still today (0.02 to 0.04 mm/yr ;  
156 *Ziegler, 1992; Bonnet et al., 2000; Goslin, 2014*), but it can be considered as negligible at the  
157 Holocene timescale (40 mm/10,000 years ; *Goslin et al., 2015*). The river system is  
158 established since the Tertiary (*Hallegouët et al., 1994*). Today, the BB is characterized by a  
159 macrotidal influence with a maximum tidal amplitude of 8 m (*Troadec and Le Goff, 1997*).  
160 Grain size analyses of modern sediments reflect specific hydrodynamic conditions mainly  
161 related to tidal currents (*Gregoire et al., 2016*). In its westernmost part, the BB is connected to  
162 the Atlantic Ocean through the “*Goulet*” (Fig. 1c), a strait of about 1.8 km wide and 50 m  
163 deep. In its easternmost part, the BB receives main freshwater supplies from the Aulne and  
164 Elorn Rivers (both contributing up to 85% of the total river discharges; *Delmas and Treguer,*  
165 *1983*), as well as from the smaller Daoulas River (Fig. 1c). BB watersheds are characterized  
166 by 2,000 km of waterways and most of their runoff flows into the BB through the Aulne River

167 (114 km long; 1,224 km<sup>2</sup> of watershed and 20.40 m<sup>3</sup>/s of annual debit; *Troadec and Le Goff,*  
168 *1997*).

169 The bathymetric map of the BB highlights submarine channels that attest to palaeo-fluvial  
170 systems (Fig. 1c; *Gregoire et al., 2016*). Palaeo-channels of the two main current rivers,  
171 Aulne and Elorn, are about 30 and 15 m deep respectively, and converge in the west at a  
172 trough of about 50 m deep (*Troadec and Le Goff, 1997*). Nevertheless, at present, the depth of  
173 the BB does not exceed 10 m deep on approximately 60% of its surface (*Monbet and*  
174 *Bassoulet, 1989*). The last transgressive episode corresponds to the complex and fragmented  
175 sedimentary infilling history of the BB (*Gregoire et al., 2017*), because of i) the non-  
176 morphological uniformity of the substratum, ii) the non-linear post-glacial sea level rise,  
177 combined with iii) strong and complex hydrodynamical features (*Gregoire et al., 2017*).  
178 Palaeo-valleys became flooded according to different steps of large fluvial terraces (*Gregoire*  
179 *et al., 2017*), considerably decreasing surfaces occupied by intertidal salt-marshes and  
180 mudflats (i.e. typical environments submitted to intertidal dynamics); the shallowest parts of  
181 the BB being flooded between 9,000 and 7,000 years BP. Today, the centre of the BB is  
182 predominantly under marine influence, main river mouths and intertidal areas having  
183 migrated further east.

184

## 185 **2.2. Climatic Context**

186 Brittany is subjected to a temperate oceanic climate regime characterized by the influence of  
187 the westerlies and by low seasonal thermal amplitudes with mean annual temperatures of  
188 about 10-11°C (*Belleguic et al., 2012*). Annual prevailing winds (with speeds that can exceed  
189 100km/h during 5 to 15 days per year) have mainly a south-west origin (*Troadec and Le Goff,*  
190 *1997*). Since Brittany is submitted to regular oceanic rainfalls, annual cumulative precipitation



191 data ranges from 600 mm/year to more than 1,600 mm/year in the inner continental part  
192 (*Troadek and Le Goff, 1997; Belleguic et al., 2012*). The climate of Brittany is due to the  
193 combined influences of atmospheric (North Atlantic Oscillation, NAO) and oceanic (Atlantic  
194 Multidecadal Oscillation, AMO) circulations detailed thereafter (*Tréguer et al., 2014,*  
195 *Ruprich-Robert and Cassou, 2015; Lambert et al., 2018*). On decadal to multi-decadal  
196 timescales, variations in North Atlantic sea-surface temperature (SST) control a large part of  
197 the climate variability reconstructed on the continent (*Deser et al., 2010; Knight et al., 2006;*  
198 *McCarthy et al., 2015; Ruprich-Robert and Cassou, 2015*), already discussed in the BB  
199 watersheds (*Lambert et al., 2018*).

200

### 201 **2.3. Cultural evolution and territorial occupation dynamics**

202 The Mesolithic is poorly documented in western Brittany due to the scarcity of archeological  
203 data. The French Mesolithic period is divided into two sub periods, the first Mesolithic (10th,  
204 9th, and 8th millennia BC) and the second Mesolithic (7th, 6th and early 5th millennia BC,  
205 depending on the studied region) according to cultural criteria based on lithic industries  
206 (*Marchand, 2014*). Across the Mesolithic, traces of shellfish consumption as well as of  
207 microlithic industries on the coastline suggest the presence of small communities irregularly  
208 spread over western Brittany (perhaps 25,000 to 50,000 people; *Giot et al., 1998*). Also, lithic  
209 material resulting from debitage has been found in Finistère (western Brittany), evidencing  
210 human settlements 20 kilometers from the current coast. Human groups may have moved  
211 seasonally between coasts, riversides and the inner land (*Gouletquer et al., 1994, 1996*), while  
212 recent studies rather suggest perennial settlements of restricted communities in some coastal  
213 areas (*Schulding and Richards, 2001; Marchand, 2005*). Previous pollen studies have not  
214 shown significant environmental impacts in Brittany due to human hunter-gatherer  
215 populations (*Morzadec-Kerfourn, 1974*).

216 The Neolithic "revolution" then reached western Europe around 5,500 BC (7,450 BP) and the  
217 Armorican Massif around 5,000 BC (6,950 BP; *Blanchet et al., 2010*) via Danubian  
218 agricultural populations, evidenced by the western extension of the Linear Pottery Culture  
219 (i.e. *Blicquy-Villeneuve-Saint-Germain, in Marcigny et al., 2010*), and particularly in  
220 Southern Finistère (*Marchand et al., 2006; Marcigny et al., 2010; Tinévez et al., 2015*)  
221 through a diffusion model estimated at 1 km/year (*Giot et al., 1998*). The contact between  
222 Mesolithic and Neolithic societies remains poorly documented, and predation practices  
223 gradually shifted to a production economy thanks to the domestication of animals and the  
224 emergence of agriculture. For many years, these cultural changes have been debated as the  
225 result of i) the acculturation of indigenous hunter-gatherer populations, or ii) a population  
226 replacement by Neolithic societies coming from the East. Recent genetic studies conducted on  
227 European populations suggest a Mesolithic population replacement, nevertheless highlighting  
228 a mosaic of *scenarii* according to regions, and a non-uniform demographic transition across  
229 Europe with few evidences of cultural adoption (*Sampietro et al., 2007 ; Bramanti et al., 2009*  
230 ; *Haak et al., 2010; von Cramon-Taubadel and Pinhasi, 2011 ; Skoglund et al., 2012*).  
231 Western Europe population increased sharply as a result of increasing food production.  
232 Perennial settlements of Neolithic villages are observed in western France from the first  
233 centuries of the 5<sup>th</sup> millennium BC (around 7,000 to 6,700 BP) (*Marchand, 2014*).

234 Considering the emergence of agriculture, palynological and palaeobotanical data are very  
235 rare in Finistère. Some studies carried out over Brittany are mainly based on lithic industries  
236 and funeral practices (*Marchand, 2005*), and the beginning of the neolithisation thus cannot  
237 be precisely dated, such as in other parts of Europe (*Kirleis et al., 2012; McClatchie et al.,*  
238 *2014*). In the coastal Morbihan (Locmariaquer, SE Brittany), *Visset et al. (1996)* suggested  
239 ancient cereal farming occurred around 7,243-5,800 BC (9,193-7,750 BP) because of cereal  
240 pollen grain occurrences in Mesolithic levels, observed concomitantly with increases of

241 ruderal plant and *Corylus* percentages, as well as a marked decrease of other arboreal pollen  
242 taxa. Other palynological studies also discussed the presence of cultivated taxa since the  
243 Mesolithic in SE Brittany and around the Loire valley (*Barbier and Visset, 1997; Ouguerram*  
244 *and Visset, 2001; Visset et al., 2002; Joly and Visset, 2005*). However, the absence of  
245 agricultural tools in archaeological sites in the direct vicinity of the above-mentioned sites did  
246 not allow confirming these assumptions based on palynological observations (*Marchand,*  
247 *2005*). Since the early Neolithic, anthropogenic environmental disturbances and evidences of  
248 cereal-cropping became more and more prevalent (*Visset, 1979; Marguerie, 1991*). In  
249 Finistère, the cereal cultivation practice is attested from 3,500 BC (5,450 BP) by the presence  
250 of cereal grains in the archeological site of Molène island (*Dréano et al., 2007*). On the other  
251 hand, human impact on the environment becomes noticeable from the first half of the 5th  
252 millennium BC with the first appearance of grindstones and more particularly with traces  
253 detected on lithic furniture typical from the cutting of plant fibers (*Giot et al., 1998; Guéret et*  
254 *al., 2014*).

## 255 **3. Material and methods**

### 256 **3.1. Study sediment cores**

257 Pictures and RX radiography were carried out at the *Géosciences Marines* laboratory  
258 (IFREMER, Plouzané, France) for the three study cores (Fig.1), and description,  
259 granulometric analyses (laser granulometer “MASTERSIZER 2000”), as well as sampling for  
260 AMS <sup>14</sup>C dates and palynological analyses were carried out at the *Géosciences Océan*  
261 laboratory (LGO-IUEM, Plouzané, France). All dates (Table 1) have been calibrated with the  
262 CALIB 7.1 program using the Marine13 calibration curve (*Stuiver and Reimer, 1993; Reimer*  
263 *et al., 2013*) and a  $\Delta R$  of  $-40\pm 23$  years (*Mangerud et al., 2006*). In the manuscript, when  
264 referred to a precise age, the mention to “Cal.” will not systematically be written, and ages in

265 “years BP” or “years BC” will often be both specified so as to facilitate the lecture of the  
 266 results for paleoenvironmental or archeological communities, respectively.

267 Within the BD, core “VC2012-08-PQP” (48°10.2’N, 04°26.4’W; 28 m depth; 486 cm length;  
 268 Fig. 1b, 3, 4) was recovered with a vibrocorer by the R/V *Pourquoi Pas?* during the Proteus-  
 269 Dunes cruise (Shom, 2012). Within the BB, core “A” (48°19.2’N, 4°31.8’W; 8.2 m depth;  
 270 418 cm length in total but 318 cm available for this study: the top 100 cm were entirely used  
 271 in 2003-2004 by biologists and bio-geochemists) was retrieved in the Bay of Roscanvel (i.e.  
 272 small bay in the western part of the BB; Fig. 1c, 5) also with a vibrocorer by the R/V *Côtes de*  
 273 *la Manche* during the “*Défis Golfe de Gascogne*” program (IFREMER, LEMAR-IUEM,  
 274 2003). Finally, core “KS-24” (48°19.3’N, 4°31.4’W; 26 m depth; 181.5 cm length) was  
 275 retrieved in the Bay of Roscanvel (BR; Fig. 1c, 5) with a gravity corer by the R/V *Thalia*  
 276 during the “*SERABEQ 3*” cruise (IFREMER, 2015).

277

Lab code	Depth (cm)	material	Age <sup>14</sup> C	Error	Age Cal. BP Min-max (mean)	Age Cal.AD/BC
<b>Core VC08</b>						
<b>Poz-85161</b>	20	Gastropod	1210	30	702-894 <b>(798)</b>	<b>1152 AD</b>
<b>SacA47754</b>	23.5	Bivalve	635	30	257-420 <b>(338.5)</b>	<b>1611.5 AD</b>
<b>SacA47756</b>	103	Bivalve	7905	45	8313-8524 <b>(8418.5)</b>	<b>6468.5 BC</b>
<b>SacA47755</b>	158	Bivalve	8025	40	8401-8628 <b>(8514.5)</b>	<b>6564.5 BC</b>
<b>SacA43117</b>	240	<i>Acanthocardia</i> sp.	8030	35	8410-8625 <b>(8517.5)</b>	<b>6567.5 BC</b>
<b>SacA43118</b>	266.5	Bivalve	8060	35	8433-8688 <b>(8560.5)</b>	<b>6610.5 BC</b>
<b>SacA43119</b>	337.5	Bivalve	8090	30	8483-8737 <b>(8610)</b>	<b>6660 BC</b>
<b>SacA49420</b>	345	Bivalve	8105	35	8492-8774 <b>(8634.5)</b>	<b>6684.5 BC</b>
<b>SacA43120</b>	375.5	<i>Bittium</i> sp.	8580	60	9091-9435 <b>(9263)</b>	<b>7313 BC</b>

<b>SacA43115</b>	405	<i>Spisula</i> sp.	8960	35	9532-9827 <b>(9679.5)</b>	<b>7729.5 BC</b>
<b>SacA43121</b>	408	<i>Ostrea</i> sp.	8950	35	9527-9810 <b>(9668.5)</b>	<b>7718.5 BC</b>
<b>Core KS24</b>						
<b>Poz-78151</b>	102.5	Gastropod	8410	50	8938-9247 <b>(9092.5)</b>	<b>7142.5 BC</b>
<b>Poz-78152</b>	173.5	Gastropod	8530	50	9045-9383 <b>(9214)</b>	<b>7264 BC</b>
<b>Core A</b>						
<b>Poz-42799</b>	18-19	<i>Venerupis senegalensis</i>	4930	35	5221-5445 <b>(5333)</b>	<b>3383 BC</b>
<b>SacA49424</b>	46	<i>Turritella</i> sp.	5390	30	5704-5899 <b>(5801.5)</b>	<b>3851.5 BC</b>
<b>SacA41585</b>	70	Bivalve	5375	30	5686-5890 <b>(5788)</b>	<b>3838 BC</b>
<b>SacA43114</b>	109-110	<i>Venus</i> sp.	5540	40	5873-6114 <b>(5993.5)</b>	<b>4043.5 BC</b>
<b>Poz-42840</b>	114.5- 116.5	<i>Venerupis senegalensis</i>	5580	35	5911-6149 <b>(6030)</b>	<b>4080 BC</b>
<b>Poz-42841</b>	161	<i>Dosinia lupinus</i>	5690	40	6005-6258 <b>(6131.5)</b>	<b>4181.5 BC</b>
<b>Poz-42842</b>	187	<i>Patia rhomboides</i>	5790	40	6159-6365 <b>(6262)</b>	<b>4312 BC</b>
<b>SacA41583</b>	190-191	Bivalve	5715	30	6059-6273 <b>(6166)</b>	<b>4216 BC</b>
<b>SacA41584</b>	<b>190-191</b>	<b>Organic matter For the reservoir age</b>	<b>5350</b>	<b>60</b>	<b>5993-6280 (6136.5)</b>	<b>4186.5 BC</b>
<b>Poz-42843</b>	229-231	<i>Venerupis senegalensis</i>	5900	40	6264-6457 <b>(6360.5)</b>	<b>4410.5 BC</b>
<b>SacA41581</b>	248-249	Bivalve	5990	30	6335-6557 <b>(6443)</b>	<b>4496 BC</b>
<b>SacA41579</b>	258	Bivalve	5960	30	6303-6508 <b>(6405.5)</b>	<b>4455.5 BC</b>
<b>SacA41580</b>	297	Bivalve	6105	30	6464-6677 <b>(6570.5)</b>	<b>4620.5 BC</b>
<b>Poz-42844</b>	316	<i>Venerupis senegalensis</i>	6155	35	6510-6744 <b>(6627)</b>	<b>4677 BC</b>

278 Table 1: carbon dates made on VC-08, A and KS-24 cores. The 190 cm level on core A, dated  
279 from continental organic matter, is not considered in the age model. It was duplicated from  
280 the level 190 cm dated on bivalve to estimate the reservoir age in the Bay of Brest.

### 281        **3.2. Palynological analyses**

282 Palynological preparations were carried out at the EPOC laboratory (University of Bordeaux,  
283 Talence), following the procedure described by *de Vernal et al. (1999)* and using chemical  
284 (cold HCl and cold HF) and physical (sieving through a 10 µm nylon mesh screen) treatments  
285 in order to remove the mineral fraction and to concentrate palynomorphs (cf.  
286 [http://www.epoc.u-bordeaux.fr/index.php?lang=en&page=eq\\_paleo\\_protocoles](http://www.epoc.u-bordeaux.fr/index.php?lang=en&page=eq_paleo_protocoles)). The final  
287 residue was mounted between slide and coverslip with glycerin. Pollen and dinocysts were  
288 determined using an optical microscope Leica DMC 2900 at X630 magnification.

289 In this study, 89 samples (46 for core “A”, 4 for core KS-24 and 39 for core VC-08) were  
290 analyzed allowing to obtain a study resolution of about 20 to 30 years. Palynomorph  
291 identification followed *Beug (1961)*, *Faegri and Iversen (1989)*, *Moore et al. (1991)* and  
292 *Reille (1995)* for pollen and *Rochon et al. (1999)* for dinocysts. For each analyzed sample, a  
293 minimum of 300 pollen grains and 150 dinocysts have been counted in order to provide robust  
294 assemblages from a statistical point of view (*Fatela and Taborda, 2002*). Percentages were  
295 calculated on a sum of total pollen grains, or a sum of total dinocysts, without any exclusion.  
296 Concentrations (number of specimens/cm<sup>3</sup>) were obtained thanks to the *Lycopodium* spore  
297 method (*Mertens et al., 2009*). Through a camera connected to the optical microscope,  
298 measurements were also performed on the size of the annulus and of the diameter of Poaceae  
299 grains along the VC-08 core so as to differentiate *Cerealia* from wild grasses (*Leroyer et al.,*  
300 *2004; Joly et al., 2007*). Finally, other palynomorphs were counted, including microalgae,  
301 foraminiferal linings, spores and copepod eggs.

302

### 303 **3.3. Foraminiferal analyses**

304 Prior to the palynological treatments, bulk sediments were sieved at 150  $\mu\text{m}$ , and the fraction  
305  $>150 \mu\text{m}$  was used for foraminiferal analyses. After dividing the largest samples with a  
306 micro-splitter, benthic foraminiferal assemblages were analyzed with a LEICA M60 binocular  
307 stereo zoom microscope at X60 magnification. Identification followed *WoRMS Editorial*  
308 *Board (2017)* ([www.marinespecies.org](http://www.marinespecies.org)). Data were expressed in percentages of total benthic  
309 foraminiferal counts (at least 100 specimens counted per level). 16 samples (12 for core “A”  
310 and 4 for core KS-24) were analyzed allowing a resolution of about 150 years.

311 Monospecific stable oxygen and carbon isotopes were also measured for core “A” on the  
312 *Elphidium aculeatum* benthic species, in the same levels than benthic foraminiferal  
313 assemblages. About five specimens were hand-picked in the 150-250  $\mu\text{m}$  sediment fraction,  
314 cleaned in a methanol ultrasonic bath for a few seconds, then roasted under vacuum at 380  $^{\circ}\text{C}$   
315 for 45 min to remove organic matter, prior to isotopic analyses (*Duplessy, 1978*). The  $\delta^{18}\text{O}$   
316 and  $\delta^{13}\text{C}$  (expressed in ‰ VPDB) were measured at the PSO (IUEM, BREST) using the  
317 IRMS platform: a Delta V mass-spectrometer coupled with a GasBench II preparation line for  
318 benthic species. The external reproducibility ( $1\sigma$ ) of an internal standard calibrated with  
319 NBS19 is  $\pm 0.03 \text{ ‰}$  and  $0.06 \text{ ‰}$  for  $\delta^{13}\text{C}$  and  $\delta^{18}\text{O}$  respectively.

## 320 **4. Sedimentary context and palynological results**

### 321 **4.1. Bay of Douarnenez, BD (core VC-08)**

#### 322 *Sedimentary facies and age model*

323 The sedimentology, granulometry and magnetic susceptibility analyses (Fig. 3, 4), core VC-  
324 08, taken from a BD palaeo-valley (Fig. 1b) highlight different sedimentary deposits that can  
325 be related to the sediment units defined in the framework of the study of the sedimentary  
326 infilling history of the BD (*Le Roy and Jouet, 2005*; Fig. 2).

327 The base of core VC-08 (from 474 to 425 cm) is made of coarse sands (mean granulometry of  
328 about 1,500  $\mu\text{m}$ ) with high magnetic susceptibility (MS) values illustrating a strong detrital  
329 terrigenous component (Fig. 4a), that can be related to units 1 and 2 (U1 and U2 of *Le Roy*  
330 *and Jouet, 2005*; Fig. 2, 4b) and interpreted as fluvial deposits during the last glacial period.  
331 Between 425 and 340 cm, granulometry oscillates from coarse silts to very fine sands marked  
332 by a large grain-size variability (from 5 to around 1,500  $\mu\text{m}$ ; Fig. 4a,b), and a fairly high  
333 concentration of broken bivalve shells, therefore probably reflecting high energetic  
334 conditions. The drop of MS values is related to major environmental change from continental  
335 to marine influences, with the sea starting to reach the westernmost part of the channels  
336 around 10,000 years BP. This interval can be associated to units 3 and 4 (U3 and U4 of *Le*  
337 *Roy and Jouet, 2005*; Fig. 2, 4b). Between 340 and 30 cm, clayey sediments (mean  
338 granulometry of 10  $\mu\text{m}$ ; Fig. 4a,b) and tidal laminae dominate sedimentary facies. After a  
339 small increase, MS values gradually decrease from 250 cm to the top (Fig. 4a). This very  
340 thick deposit constitutes most of the sedimentary infilling of BD channels and corresponds to  
341 unit 5 (U5 of *Le Roy and Jouet, 2005*; Fig. 2, 4b). The last sedimentological deposit (30 cm  
342 upwards), delimited at its base by an erosive surface, is characterized by marine sands (mean  
343 granulometry of 100  $\mu\text{m}$ , three main modes between 10 and 1,000  $\mu\text{m}$ ; Fig. 4a,b) reworked  
344 and remobilized under the action of waves. Extremely low MS values suggest the scarcity of  
345 fluvial detrital inputs within the bay. This deposit is related to the last unit 6 (U6 of *Le Roy*  
346 *and Jouet, 2005*; Fig. 2, 4b).

347 Radiocarbon dates have been obtained on bivalve and gastropod shells (Table 1). The age  
348 model (Fig. 6a) was then established from two linear regressions and 9 stratigraphic pointers  
349 considering two parts obviously distinct considering the description of the core (Fig. 4b, 6a).  
350 A significant change in sedimentation rates is therefore observed around 8,600 years BP (i.e.  
351 340 cm), related to the Holocene sedimentary infilling history, with 0.06 cm/yr calculated



352 before 8,600 years BP and 1.2 cm/yr calculated after (Fig. 4, 6a). Two additional dates  
353 obtained in the uppermost part of the core (i.e. 20 and 23.5 cm, 798 and 338.5 BP,  
354 respectively; Fig. 4b) confirm the recent set up of the last unit made of reworked marine sands  
355 (U6 in *Le Roy and Jouet, 2005*). These two dates were therefore not used to build the age  
356 model (Fig. 6a). The palynological study is conducted on the fine intertidal sedimentation  
357 section of the core, corresponding to units U4 and U5 described by *Le Roy and Jouet (2005)*  
358 (Fig. 3, 4b) and ranging from 390 to 30 cm (i.e. 9,400 to 8,400 years BP or 7,450 to 6,450  
359 years BC), thus providing information on the final Mesolithic.

360

### 361 **Dinocysts**

362 A total of 18 taxa were recognized with an average of nine different taxa per slide. Only main  
363 taxa (i.e. greater than 2 % at least once in palynological spectra) were plotted on Fig. 7a along  
364 with concentrations (cysts/cm<sup>3</sup>) and specific richness (number of different taxa per slide).  
365 Taken as a whole, *Spiniferites bentorii* (50 % in average) and *Lingulodinium*  
366 *machaerophorum* (11 %) are the most abundant taxa as it is usually described on Brittany's  
367 coasts (*Morzadec-Kerfourn, 1977; Lambert et al., 2017*). The variations of the dinocyst  
368 assemblages enable to highlight three main zones, with very low diversity values at the base  
369 of the record (VC-A, 390-345cm), followed by a slow increase up to 250 cm (VC-B, 345-250  
370 cm), and higher values over the entire second half of the core (VC-C, 250-30 cm). Diversity  
371 then shifts from around 5 to 12 different taxa per slide. In addition to the low dinocyst specific  
372 richness, VC-A palynozone is defined by atypical elevated percentages of *Achomosphaera*  
373 spp., suddenly replaced by *S. bentorii*. The VC-A / VC-B boundary is well marked in dinocyst  
374 assemblages by the occurrences of *Spiniferites mirabilis*, *Spiniferites ramosus* and *Spiniferites*  
375 *delicatus*. Moreover, palynozone VC-B corresponds to increasing percentages of *L.*  
376 *machaerophorum* and a slow decrease of *S. bentorii* ones. Finally, palynozone VC-C

377 corresponds to a disappearance of *S. mirabilis* simultaneously observed with decreasing  
378 percentages of *Selenopemphix quanta*, and the first occurrence of *Spiniferites lazus* found in  
379 the study core (Fig. 7a). Moreover, these biozones are highly related to the variations of  
380 dinocyst concentrations.

### 381 Pollen

382 A total of 33 taxa were recognized with an average of 12 different taxa per slide. This rather  
383 low diversity due to the forest taxa dominance differs from the greater diversity observed in  
384 more recent Bay of Brest pollinic sequences (e.g. Lambert *et al.*, 2017, 2018) and resulting  
385 from the herbaceous diversification accompanying the significant anthropogenic landscape  
386 opening. In addition to the taxa characterized by percentages found at least once above 2% in  
387 assemblages, some scarce but meaningful elements of the vegetation (i.e. *Alnus*, *Cerealia*-  
388 type) are plotted on Fig. 7b. In general, percentages of tree pollen grains are relatively stable  
389 then representing the most abundant vegetation group (average of 90 %). They are  
390 predominantly represented by *Quercus* (42 %) and *Corylus* (33 %), both taxa being then  
391 logically anti-correlated all along the core, and accompanied by low percentages of *Pinus*,  
392 *Ulmus*, *Betula* and *Alnus*. Among herbaceous plants, Chenopodiaceae are clearly dominant (7  
393 %) as well as Poaceae (2 %).

394 The overall diagram displays weak variations along the core except for total pollen  
395 concentrations and diversity that allow identifying two parts corresponding first to both VC-A  
396 and VC-B palynozones described from the dinocysts (that we will refer to palynozone VC-  
397 A&B in the following description) and, second, to VC-C palynozone (Fig. 7b). The limit  
398 between VC-A&B and VC-C is more specifically marked by a sharp increase in pollen  
399 concentrations and specific richness. Palynozones VC-A&B also correspond to a decreasing  
400 trend of *Corylus*, correlated to a *Pinus* increase, then replaced by *Quercus*. In parallel, the  
401 pollen specific richness tends to increase. The palynozone VC-C is marked by oscillations of

402 the two major taxa, *Corylus* and *Quercus*, up to 30%, contrasting with the lower part of the  
403 diagram. Concentration peaks (dotted lines in Fig. 7b) correspond to increases of *Corylus*  
404 percentages and related decreases of *Quercus* ones. In addition, a decrease of *Ulmus* is  
405 noticed throughout the sequence, along with a slight increase of herbaceous plants (e.g.  
406 Poaceae, Asteraceae, Brassicaceae). Also, *Cerealia*-type are more pronounced in palynozone  
407 VC-C. We can note again the overlap between biozones and variations in pollen  
408 concentration, as for dinocysts.

409

#### 410 **Towards a Holocene sedimentary infilling history reconstruction of the BD**

411 The sedimentological and palynological analyses conducted on core VC-08 (depicted in depth  
412 in Fig. 7 and in age in Fig. 8) allow to clarify the sedimentary infilling model discussed by  
413 *Jouet et al. (2003)* and *Le Roy & Jouet (2005)*.

414 From 474 to 420 cm (Fig. 4b), sediments are too coarse to be sampled for palynological  
415 analysis. This part could be related to the bedrock incision by rivers during the end of the last  
416 glacial period (U1 and U2; Fig. 2), as also evidenced in our study by high magnetic  
417 susceptibility (MS) values (Fig. 4a). Palynological results highlight a high Pollen/Dino ratio  
418 from 390 to 340 cm (8,630 years BP) (palynozone VC-A; Fig. 8) suggesting a major pollen  
419 contribution of surrounding watersheds and therefore predominant fluvial *versus* marine  
420 inputs, corresponding then to the fluvial deposits (fluvial accretion bars of U3-U4 in *Le Roy*  
421 *and Jouet, 2005*; Fig. 2 and 4b). The Chenopodiaceae content (Fig. 7b) is likely a clue of the  
422 already settled salt-marshes. Still discrete marine influences do not allow dinoflagellates to  
423 occur in large number during palynozone A, the study core being located upstream in the  
424 palaeo-river network incising the substratum of the BD (Fig. 1b). Unfortunately, the ecology

425 of *Achomosphaera* spp. is not precisely known and the taxa thus cannot be connected to  
426 particular ecological conditions at that time.

427 From 340 to 250 cm (8,630 to 8,550 BP, palynozone VC-B, Fig. 7 and 8, lower part of U5 in  
428 Fig. 4b) the marine influence is first marked by the increased dinocyst diversity, including  
429 euryhaline taxa such as *L. machaerophorum* and *S. belerius*, together with taxa more  
430 characteristic of marine environments such as *O. centrocarpum*, *S. delicatus*, *S. mirabilis* and  
431 *S. ramosus* (Morzadec-Kerfourn, 1977, 1979). In parallel, decreasing percentages of the  
432 typically coastal species *S. bentorii* is probably more related to increasing percentages of the  
433 other taxa. The lower part of U5 corresponds to a thick transitional sequence between  
434 continental and marine influences, submitted to the relative sea-level rise as observed through  
435 the continuous decrease of the Pollen/Dino ratio (Fig. 8). The already mentioned breakdown  
436 in sedimentation rates at 340 cm (limit between U4 and U5; Fig. 4, 6a) corresponds to this  
437 major transition towards an estuarine sedimentation. Variations in particle size and in  
438 sediment facies are also obvious through the sudden jump in MS values, indicating greater  
439 continental intakes from 8,600 years BP (Fig. 4a, 10).

440 From 250 cm (palynozone VC-C in Fig. 7 and 8, U5 upper part in Fig. 4b), marine influences  
441 are well established with a low Pollen/Dino ratio (Fig. 8), a high dinocyst diversity and the  
442 persistence of typically coastal (i.e. *S. bentorii*) and marine (i.e. cysts of *P. dalei*, *O.*  
443 *centrocarpum*, *S. membranaceus*, *S. delicatus*) dinocyst taxa, already observed in the previous  
444 zone (Fig. 7a). *L. machaerophorum*, often associated to fluvial and estuarine brackish  
445 environments (Marret and Zonneveld, 2003), displays percentages that exceed the average of  
446 its whole dataset (Fig. 7a) and are anti-correlated with *S. bentorii* and/or *O. centrocarpum* (i.e.  
447 more related to the oceanic domain; Morzadec-Kerfourn, 1976, 1979) ones.

448 Palynological studies conducted on core VC-08 therefore confirm the environment sketches  
449 proposed by *Le Roy and Jouet (2005)* on the basis of sedimentological and seismic data.  
450 Furthermore, an obvious major limit can be defined within the tidal facies of U5 at 8,550  
451 years BP, with a lower transitional part under increasing marine influences, and an upper part  
452 characterized by well-established marine conditions in a perennial flooded bay.

453

#### 454 **4.2. Western Bay of Brest (A and KS-24 cores Bay of Roscanvel)**

##### 455 **Sedimentary facies**

456 Core “A” (Fig. 5a) is characterized by clayey sediments and numerous shell debris (Fig. 5b)  
457 as well as bivalve and gastropod shells in life position often sampled for dating. The age  
458 model (Fig. 6b) was established through a linear regression between 13 AMS  $^{14}\text{C}$  dates (Table  
459 1) allowing to consider an interval of about 1,400 years (6,700 to 5,300 BP or 4,750 to 3,350  
460 BC) and mean sedimentation rates of about 0.26 cm/yr (Fig. 6b). Palynological analyses have  
461 been conducted along the 318 cm of the core. It is worth noting that in one sample, the 190-  
462 191 cm level (Table 1), continental organic matter (vegetal fibers) has been dated in parallel  
463 with a bivalve for obtaining an estimation of the age reservoir within the Bay of Brest. When  
464 calibrating the  $^{14}\text{C}$  ages with IntCal13 without assuming any age reservoir effect on the  
465 marine carbonate material, we obtain a difference of about 357 years between both dates, thus  
466 indicating a  $\Delta\text{R}$  of -43 years, very close to the one calculated by *Mangerud et al. (2006)* off  
467 the Sein Island (i.e.  $\Delta\text{R}$  of  $-40\pm 23$  years) (<http://calib.org/marine/>).

468 Regarding core KS-24 (Fig. 5a), sampled in a deeper but closed site, the basal part is  
469 characterized by clayey sediments sampled for palynological analyzes, and the upper part  
470 consists in coarse sands and shell debris (Fig. 5c). These two parts of the core are separated by  
471 a well-marked erosive surface at around 100 cm depth. Two AMS  $^{14}\text{C}$  dates carried out at

472 173.5 and 102.5 cm allow dating the clayey section (i.e. interval sampled for palynological  
473 analyzes; Fig. 5c) between 9,214 and 9,092 years BP (7,264 and 7,142 years BC).

474

#### 475 **Dinocysts**

476 In both cores, 24 different taxa were identified, with an average of three different taxa per  
477 slide for core KS-24 and 12 for core “A”. Similar to core VC-08, only main taxa were plotted  
478 on Fig. 9a along with dinocyst concentrations and the specific richness. These two cores  
479 constitute two temporal windows (i.e. 9,200-9,000 years BP for core KS-24, and 6,700-5,300  
480 years BP for core “A”) on the same study site (i.e. Bay of Roscanvel, westernmost part of the  
481 Bay of Brest; Fig. 1c). Both cores are described together, in their stratigraphical order, core  
482 KS-24 representing a palynozone by itself.

483 Core KS-24 is characterized by the largely dominant *S.bentorii* species (69 %; Fig. 9a),  
484 similar to the BD at the same period (Fig. 7a). Co-occurring with cysts of *P. dalei*, *O.*  
485 *centrocarpum*, *S. membranaceus* and *S. quanta* at the base, *S. bentorii* becomes monospecific  
486 at the top of core KS-24. From the base to the top of core “A”, dominant taxa are first  
487 characterized by cysts of *P. dalei*, then replaced by *L. machaerophorum* that reach about 80  
488 %. Decreasing percentages of cysts of *P. dalei* and *S. ramosus* are consequently observed at  
489 the same time. Variations in percentages of major species and in total concentrations allow us  
490 to delimit three palynozones (two of them being subdivided in two sub-palynozones). First  
491 palynozone A-A (from 318 to 250 cm, Fig. 9a) displays a significant increasing trend of cysts  
492 of *P. dalei*, a decreasing trend of *L. machaerophorum* and high percentages of *S. ramosus* and  
493 *S. membranaceus*. At the limit between A-A and A-B, total cyst concentrations as well as *L.*  
494 *machaerophorum* percentages show their lowest values, while cysts of *P. dalei* reach its  
495 highest percentages (i.e. around 50 %). Second palynozone A-B (250-100 cm) is well marked  
496 by noticeable opposite trends, and especially by increasing percentages of *L.*

497 *machaerophorum* and decreasing ones of cysts of *P. dalei*. Then *S. bentorii* displays higher  
498 values than in the previous zone, while *S. ramosus* displays lower percentages. Moreover,  
499 palynozone A-B corresponds to the strongest occurrences of *S. lazus*. This palynozone has  
500 been divided into two sub-palynozones. Within zone A-B1, *L. machaerophorum* percentages  
501 are the lowest while those of cysts of *P. dalei* are the highest of their respective whole  
502 datasets. *L. machaerophorum* occurrences gradually rise in zone A-B2 and *S. bentorii*  
503 percentages stabilize with a plateau of high percentages during this interval. The third  
504 palynozone A-C (from 100 cm onwards; Fig. 9a) corresponds to a huge increase of *L.*  
505 *machaerophorum* percentages while those of cysts of *P. dalei* sharply decrease, together with  
506 a drop of *S. ramosus*. An additional subdivision is proposed to highlight the abrupt increase in  
507 dinocyst concentrations at 50 cm (limit between A-C1 and AC-2). Furthermore, within zone  
508 A-C1, weak but significant occurrences of *S. membranaceus* and *S. mirabilis* are observed,  
509 while percentages of cysts of *P. dalei*, *S. mirabilis*, but also *S. ramosus*, and *S. lazus* drop to  
510 extremely low values within zone A-C2. Conversely, *O. centrocarpum* and *S. belerius* slightly  
511 increase in last zone A-C2.

512

### 513 **Pollen**

514 In both cores, 34 different taxa were recognized with an average of 11 different taxa per slide  
515 for core KS-24 core and 12 for core “A” (Fig. 9b). While the two major taxa are the same for  
516 both cores (i.e. *Corylus* and *Quercus*), pollen concentrations are much higher in core KS-24  
517 (9,200-9,000 years BP) than in core “A” (6,700-5,300 years BP). Furthermore, trees are much  
518 more present in core “A” than in the core “KS-24 (i.e. 93 % vs. 79 %). Among the herbaceous  
519 in the core KS-24, Chenopodiaceae are particularly represented with an average of 12 %.

520 In core “A”, increasing percentages of *Alnus* (from 0 % to 15 %), and decreasing trends of  
521 *Ulmus* and *Tilia*, allow to delimit the same palynozones than those described for dinocysts  
522 (Fig. 9a). In general, herbaceous plants are very rare but a slow diversification is observed  
523 towards the top, with the appearance of some minor taxa (e.g. Ranunculaceae, *Mercurialis*,  
524 *Plantago* spp., Caryophyllaceae). *Corylus* and *Quercus* are anti-correlated throughout the  
525 core. More specifically, the first palynozone A-A (318 to 250 cm; Fig. 9b) corresponds to low  
526 percentages of *Corylus* that gradually increase at the end of the palynozone and, conversely,  
527 to high percentages of *Quercus* that tend to gradually decrease. During this interval, *Tilia* and  
528 Poaceae represent a meaningful part of the pollen content. Second palynozone A-B (250 to  
529 100 cm) displays the occurrence and rise of *Alnus*, as well as the noticeable decrease of both  
530 Poaceae and *Tilia*. Furthermore, at the start of palynozone A-B, *Ulmus* and *Pinus* percentages  
531 exhibit stable values when compared with palynozone A-A, while they suddenly drop around  
532 200cm, allowing to discriminate sub-palynozones A-B1 (from 250 to 200 cm) and A-  
533 B2 (from 200 to 100 cm). Conversely, *Alnus* percentages strongly increase in sub-palynozone  
534 A-B2. Palynozone A-C (from 100 cm onwards) highlights a new threshold with a marked  
535 decrease of *Ulmus* together with a strong increase in *Alnus* percentages, the latter reaching its  
536 highest values within zone A-C2 in parallel with relatively continuously high pollen  
537 concentrations. Interestingly, most of the main peaks observed with pollen concentrations  
538 (dotted lines in Fig. 9b) also correspond to increases of *Alnus* percentages along with high  
539 values of *Corylus*, as already noticed for the VC-08 record.

540

#### 541 **Micropalaeontological results**

542 Benthic foraminiferal assemblages are presented in depth for cores “A” and KS-24 (Fig. 10),  
543 in parallel to the isotopic data measured on *Elphidium aculeatum*. Since *Elphidium* spp. are  
544 the dominant taxa, all other taxa percentages have been calculated on a main foraminiferal



545 sum that excludes *E. crispum* and *E. aculeatum*. Similar to palynological data, only species  
546 occurring at least once with percentages above 2% have been plotted in Fig. 10.

547 Along core KS-24, foraminiferal concentrations are low and assemblages are dominated by  
548 *Haynesina germanica* (average of about 50 %), with few *Elphidium* spp. and important  
549 variations of *Ammonia* spp., here strictly assigned to the species *A. tepida*.

550 Along core A, an increase of total benthic foraminiferal concentrations is observed throughout  
551 the sequence and epifauna are the most represented in benthic foraminiferal assemblages, with  
552 *Elphidium aculeatum* and *E. crispum* both accounting for 70%. Zones previously described  
553 for dinocysts and pollen grains have been reported in the foraminiferal diagram, so as to  
554 facilitate the cross-correlated approach between all fossil bio-indicators. Zone A-A is mainly  
555 characterized by *Elphidium* spp. that displays an increasing trend, an important content of  
556 Miliolidae, and an abrupt decrease of *Cibicides* spp. In addition, *Ammonia tepida* and  
557 *Planorbulina mediterranensis* are observed with significant percentages. Palynozone A-B  
558 corresponds to still high *Elphidium* spp. percentages and occurrences of *A. becarii*. Within  
559 this interval, two subzones correspond first (i.e. A-B1, 250 to 200 cm) to decreasing values of  
560 *Cibicides* and Miliolidae, together with the occurrence of *Lagena* spp., and then (i.e. A-B2,  
561 200 to 100 cm) to increasing percentages of *Cibicides* (reaching 20%) and drastically low  
562 *Lagena* percentages. Within palynozone A-C (from 100 cm onwards), *A. becarii* is replaced  
563 by *A. tepida*, while *Cibicides* spp., *P. mediterranensis* and epiphytes (i.e. with a flat face that  
564 allow them to be attached to sediments or plants) show approximately a same increasing  
565 profile, opposite to the *Elphidium* spp. trend.

566 Regarding isotopic analyzes (Fig. 10),  $\delta^{13}\text{C}$  and  $\delta^{18}\text{O}$  show opposite trends with a slight  
567 decrease towards lighter values for the  $\delta^{18}\text{O}$  signal (amplitude of 1‰ between minimal and  
568 maximal values in the dataset, ranging from 1.8‰ to around 0.8‰), and a slight increase

569 towards heavier values for the  $\delta^{13}\text{C}$  signal (amplitude of 2‰ between minimal and maximal  
570 values in the dataset, ranging from -1.5‰ to around 0.5‰).

571

### 572 **Environmental evolution in the Bay of Roscanvel (BR) under the rising sea level influence**

573 Environments of the BR were greatly impacted by the relative sea-level rise between 9,000  
574 and 5,000 years BP. The general palaeoenvironmental evolution of the BR can be  
575 reconstructed thanks to two Holocene windows obtained on core “A” (6,700-5,400 years BP)  
576 and core KS-24 (9,200-9,090 years BP) and with averaged palynological (pollen and  
577 dinocysts) and foraminiferal results compiled in pie charts (Fig. 11).

578 Throughout core KS-24, dinocyst assemblages show a low general diversity with major  
579 occurrences of *S. bentorii* (Fig. 9a, 11), arguing for a strictly coastal environment. Among  
580 pollen assemblages (Fig. 9b, 11), core KS-24 displays an important content of *Corylus*, a  
581 species considered as pioneer during the post-glacial temperate forest (mixed oak) reconquest  
582 that mainly marked north-western European landscapes around 9,000 years BP (Huntley,  
583 1993; Tinner and Lotter, 2001). Among herbaceous plants, Chenopodiaceae are significantly  
584 present, certainly coming from nearby salt-marshes. In addition, foraminiferal assemblages  
585 are dominated by *Haynesina germanica*, *Ammonia tepida*, and *Elphidium williamsoni*. *A.*  
586 *tepida* and *E. williamsoni* are closely related to intertidal sheltered mudflat environments,  
587 while *H. germanica* is related to continental organic matter inputs (Debenay et al., 2006;  
588 Rossi et al., 2011). These three species indicate a highly tidal-influenced environment and  
589 local small runoffs rich in continental organic matter (Redois, 1996; Debenay et al., 2006;  
590 Perez-Belmonte, 2008; Rossi et al., 2011). However, the noticeable absence of *L.*  
591 *machaerophorum* and *Alnus* suggests low major freshwater supplies. The surrounding  
592 continental context may then correspond to small watersheds, while the Aulne River was still

593 flowing to the north of core KS-24 location taking into account the low sea level position at  
594 that time (i.e. -26 m; *Gregoire et al., 2017*; Fig. 11). In this context, the marine influence  
595 remains confined to the axis of the main channels of the Aulne and Elorn Rivers (*Gregoire et*  
596 *al., 2017*). The higher river terraces (i.e. where core “A” was taken; Fig. 1c, 5c) are entirely  
597 emerged at that time, while the lower site where core KS-24 has been retrieved (Fig. 1c, 5c) is  
598 characterized by the development of abundant maritime marshes (schorre and slikke) with  
599 halophilous plants (i.e. *Chenopodiaceae*) and a rather weak fluvial dynamic. Considering the  
600 current 26 m depth location of core KS-24 and its 1.81 m length, it allows deducing a relative  
601 sea-level between 27 and 28 meters under the current sea-level which is very similar to the 26  
602 meters proposed at 9,000 years BP by *Gregoire et al. (2017)*, taking into account the  
603 macrotidal context of north-western Brittany.

604 Throughout core “A”, dinocyst assemblages display a general higher diversity than in core  
605 KS-24 with 24 taxa, mostly oceanic to coastal, along with occurrences of about 35% of *L.*  
606 *machaerophorum* (estuarine taxon). Predominant marine influences, favorable for diversified  
607 dinoflagellate blooms, are associated to the BR marine flooding in a context of superimposed  
608 fluvial influences, as evidenced by *L. machaerophorum*, mainly associated to Aulne River  
609 inputs, here perceptible compared to the previously marsh environment described with core  
610 KS-24. Concerning pollen assemblages, the mixed temperate forest is settled (90 % of tree  
611 pollen grains, Fig. 9b and 11) with a higher representation of *Quercus* when compared to core  
612 KS-24. This indicates a connection of the BR to the main stream of the Aulne River due to the  
613 flooding of the BB, thus highlighting a more regional signature (i.e. BB watersheds) in core  
614 “A”, also corresponding to the colonization of temperate tree taxa in western Europe during  
615 the mid-Holocene (*Ruddiman and McIntyre, 1981*; *Brewer et al., 2002*). The *Chenopodiaceae*  
616 signal is less pronounced in core “A” due to the disconnection of the study site from marsh  
617 environment, as also confirmed by the drastic reduction in marsh-related foraminiferal species

618 (i.e. *Haynesina germanica*, *Ammonia tepida*, and *Elphidium williamsoni*). Also, benthic  
619 foraminiferal assemblages display a stronger diversity in core “A” suggesting a greater marine  
620 influence in agreement with dinocyst results. Moreover, the presence of some epiphytic and  
621 fixed species (i.e. *Cibicides* spp. and *Planorbulina mediterraneensis*) suggests a higher  
622 hydrodynamism. In addition, the absence of benthic infauna could indicate a lack of very  
623 important organic matter inputs. The environment would therefore be characterized by a  
624 sufficient organic matter supply to allow the development of algal coverings (allowing the  
625 presence of epiphytes), and hydrodynamism would disperse this organic material, thus  
626 oxygenating the bottom. In summary, around 6,000 years BP the relative sea level was  
627 relatively close to the present-day one (*Goslin et al., 2015*) and the BB as a whole (and thus  
628 the BR) is flooded (Fig. 11). The environment is then marked by a clearer marine influence  
629 and the remoteness of salt-marshes areas. Tidal currents erode sediments on terrace slopes  
630 from the main channels, leading to erosive surfaces separating muddy and sandy facies (i.e.  
631 upper part of KS-24 core from 100 cm onwards not sampled for palynological analysis, Fig.  
632 5c), as also identified by *Gregoire et al. (2017)*.

633

## 5. Climate impacts and land-use changes

### 5.1. Local imprints of the 9,000-8,000 and 6,000-5,000 years BP RCC events

Superimposed on the palaeoenvironmental reconstitutions discussed in the context of the rising sea-level context, climate trends are well expressed in our palynological records due to our high resolution study carried out on cores characterized by high sedimentation rates.

In the Bay of Douarnenez, from 8,550 to 8,400 years BP (zone VC-C; Fig. 7b and 12), *Corylus* becomes clearly dominant. Moreover, this interval displays a slight decrease of *Ulmus*, a disappearance of the thermophilous taxon *S. mirabilis*, and significant occurrences of *S. lazus*, a dinocyst associated with cold SST (Zonneveld *et al.*, 2013). These palynological evidences may support a cooling event. Indeed, this cooling associated with the appearance of a strong seasonal contrast between 8,855 and 8,000 years BP observed by Naughton *et al.* (2007) favors the development of *Corylus* woodlands and contributes to the decrease of deciduous *Quercus* forest expanse. In the same time, the obvious increase of pollen fluxes, coeval with a marked increase of *L. machaerophorum* percentages, and *Alnus* ones to a lesser extent, may argue for increasing fluvial discharges (as previously discussed in Lambert *et al.* 2017) and thus of humidity. It is worth noting that low percentages of *Alnus* may here be ascribed to its later settlement in the vegetal reconquest succession, as observed in the Armorican Massif by David (2014). Each *L. machaerophorum* increase (Fig. 7a and 12), also concomitant to the withdrawal of coastal (*S. bentorii*) and marine (*O.centrocarpum*) species, coincides with increasing percentages and concentrations of *Corylus* (Fig. 7b and 12).

In the Bay of Roscanvel, dinocyst assemblages were dominated by *S. ramosus* (oceanic taxa; Morzadec-Kerfourn, 1977) and cysts of *P. dalei* before 6,000 years BP, and are characterised after this limit (between zones A-B and A-C) by an obvious and sharp increase of *L. machaerophorum* percentages from 30 to 70 % (Fig. 9a and 12), a species usually

658 encountered in estuarine and fluvial environments of Brittany's coasts (*Morzadec-Kerfourn,*  
659 *1977*). This could emphasize the establishment of stratified waters related to increasing fluvial  
660 inputs. Furthermore, *L. machaerophorum* is accompanied by increasing percentages of the  
661 heterotrophic taxa *S. quanta* (Fig. 9a) that could support increasing fluvial nutrient inputs to  
662 the BB. Moreover, since *Alnus* began to appear on the territory, we now observe an increase  
663 of this tree in parallel with *L. machaerophorum*. As previously observed for core VC-08,  
664 *Corylus* increases are concomitant with peaks of pollen concentrations and of *L.*  
665 *machaerophorum* percentages. Finally, higher percentages of *H. germanica* and *A. tepida*  
666 (Fig. 10), benthic foraminiferal species subordinate to environments under fluvial influences  
667 (*Debenay et al. 2006; Perez-Belmonte, 2008; Estournès et al. 2012*), confirm previous  
668 observations of increasing fluvial discharges probably related to increasing moisture.

669 For both cores VC-08 and "A", increasing fluvial inputs would correspond to a local detection  
670 of the large-scale Holocene millennial-scale climatic variability (i.e. "Bond events", *Bond et*  
671 *al. 2001*; or RCC for "Rapid Climate Change", *Mayewski et al., 2004*). Most of these cold  
672 Holocene events, initially identified in North Atlantic sedimentary cores by detrital grains  
673 drained by glaciers (Fig. 12a), correspond to Scandinavian glacier advances (*Nesje et al.,*  
674 *2001*), colder northern hemisphere temperatures and drier conditions in the tropics (*Mayewski*  
675 *et al., 1997, 2004; Meeker and Mayewski, 2002*). Also, the strengthening of the westerlies  
676 (*Bradbury et al., 1993; Mayewski et al., 2004*) may have resulted in recurrent positive modes  
677 of the NAO, leading to increased precipitations in north-western Europe. Interestingly,  
678 *Mojtahid et al. (2013)* associated the 6,000-5,000 interval to persistent positive NAO  
679 conditions in the Bay of Biscay. A solar irradiance decline may be responsible for this 6,000-  
680 5,000 years BP event (*Steinhilber et al., 2009; Fig. 12a*), also leading to a North-Atlantic SST  
681 decrease (*Jiang et al., 2015; Fig. 12a*). Thus, cores VC-08 around 8,550 years BP, and core  
682 "A" around 6,000 years BP (Fig. 12c), may then evidence for the first time the regional

683 imprint in western Brittany's coasts of two RCC events through significant increases in  
684 moisture and fluvial discharges.

685

## 686 **5.2. Local signal of *Cerealia*-type pollen grains during the Mesolithic: coastal Poaceae or** 687 **early traces of a proto-agriculture?**

688 Between 8,600 and 8,300 years BP, VC-08 core shows a very homogeneous laminated  
689 facies which attests to a stable environment aggradation related to a deltaic alluvial plain  
690 characterized by intertidal regimes (*Le Roy and Jouet, 2005; Fig. 4*). Constant percentages of  
691 Chenopodiaceae all along the record, associated with few and constant percentages of  
692 Poaceae (*Fig. 7b*), suggest a coastal marsh (slikke and schorre-type) environment, confirming  
693 the aggradation of intertidal deposits. In this sedimentary context, the palynological analysis  
694 interestingly records iterative occurrences of large pollen grains of Poaceae (*Fig. 13*).

695 Cereal pollen identifications are usually based on the diameter criteria (grain and *annulus*)  
696 following *Beug (1965), Leroyer et al. (2004)* and *Joly et al. (2007)*, because of the  
697 impossibility to separate wild grasses and *Cerealia*-type pollen grains using exine sculpture  
698 types (*Beug, 2004*). In western Europe, the commonly accepted thresholds of 45  $\mu\text{m}$  for the  
699 grain diameter and 8  $\mu\text{m}$  for its *annulus* (that we will refer as the 45-8  $\mu\text{m}$  criteria)  
700 theoretically enable the distinction between cereal pollen grains and those of indigenous wild  
701 grasses from the French western Atlantic coast (*Leroyer et al., 2004*). Considering these  
702 criteria along the whole sequence, 7 levels delivered cereal-type grains with one to 3  
703 occurrences in palynological slides. These 12 large pollen grains recognized in total, and  
704 distributed all along the core (325, 295, 220, 170, 140, 120 and 65 cm, *Fig. 13*), have been  
705 carefully measured, providing average values of 46  $\mu\text{m}$  for the grain diameter and 9.9  $\mu\text{m}$  for  
706 the *annulus*. Nevertheless, the "45-8  $\mu\text{m}$ " criteria have been criticized (*Joly et al., 2007*). The

707 statistical study conducted by *Joly et al. (2007)* on modern plants from the Atlantic coast  
708 reveals that a “45-10  $\mu\text{m}$ ” criteria makes it possible to identify 91 % of cereals (but 9 % of  
709 pollen grains are from wild grasses). In their study, *Joly et al. (2007)* then proposed to  
710 increase the thresholds to a most discriminant level of “47-11  $\mu\text{m}$ ”, thus avoiding to consider,  
711 as much as possible, larger pollen grains of coastal grasses from the Atlantic coast. The “47-  
712 11  $\mu\text{m}$ ” criteria then make it possible to discriminate 96% of cereal pollen grains (i.e. 4% of  
713 wild poaceae fall within this criterion) (*Joly et al., 2007*). However, with these new criteria,  
714 the sensibility to detect *Cerealia* pollen grains significantly declines. More precisely, among  
715 100 modern *Cerealia* pollen grains, only 59 would be detected as such with the “47-11  $\mu\text{m}$ ”  
716 criteria, the other grains being then supposed as wild Poaceae. Despite this low sensibility and  
717 the fact that some cereals are probably not taken into account with these thresholds, the  
718 applied “45-11  $\mu\text{m}$ ” criteria to our data confirm discreet peaks of *Cerealia*-type pollen grains,  
719 from around 8,600 to 8,300 years BP (at 65, 120 and 170 cm; Fig. 13).

720       Considering that indigenous coastal grasses may have larger pollen grains than continental  
721 species, it is also worth noting that these weak occurrences observed in the BD record do not  
722 co-occur in parallel with variations of other Poaceae or Chenopodiaceae, suggesting no  
723 significant changes in landscape and/or pollen transport at that time. Moreover, to be more  
724 confident about these atypical and early observations, many other clues must be considered.  
725 Some plants often associated with crops (e.g. adventitious taxa) are necessary to discuss  
726 anthropogenic signatures in the vegetation cover (*Behre, 1981; Willcox, 2005*). It is precisely  
727 interesting to note that slight increases in *Plantago lanceolata*, *Rumex* sp. and Brassicaceae  
728 percentages are observed in VC-08 core during main occurrences of *Cerealia*-type (Fig. 8 and  
729 14). A slight long-term decrease can also be highlighted in tree percentages between 8,600  
730 and 8,300 years BP, perhaps arguing for an early start of a small human-made landscape  
731 opening (Fig. 8 and 14).



732 Our findings are however in marked opposition with the regional neolithisation model  
733 admitted by the archaeological community and based on clues related to changes in cultural  
734 practices identified by lithic (and ceramic) industries (*Cassen et al., 1998; Marchand, 2005,*  
735 *2007; Marchand et al., 2006; Blanchet et al., 2006; Paillet et al., 2007, 2014; Hamon, 2008*).  
736 In addition, studies on Mesolithic archeological sites in Brittany have highlighted traces of  
737 plant cuttings, but tools did not show the classical polishes associated with cereal cuttings  
738 (*Guéret, 2013; Guéret et al., 2014*). Even if our results raise questions and encourage caution,  
739 they are consistent with other palynological studies carried out in western France that also  
740 evidenced early discreet appearances of *Cerealia*-type pollen grains (Fig. 15). As early as  
741 1996, analyses conducted by *Visset et al.* opened the debate about the existence of a very  
742 ancient cereal farms as highlighted by low occurrences of *Cerealia*-type pollen between 7,200  
743 and 5,800 years BC (9,200-7,800 years BP), concomitantly with increases of *Corylus* and  
744 ruderal plant percentages and decreasing *Quercus* percentages in the coastal Morbihan region  
745 (SE Brittany; Fig. 15). Other studies along the Loire River revealed the presence of cereal  
746 pollen taxa as well as *Juglans* between 6,400 and 5,900 years BC (8,400-7,900 years BP;  
747 *Ouguerram and Visset, 2001*) and between 6,600 and 5,800 years BC (8,500-7,800 years BP;  
748 *Carcaud et al., 2000*). Moreover, *Joly and Visset (2005, 2009)* reported cereal and ruderal  
749 pollen grains on the southern Atlantic coast (Vendée) between 7,500 and 6,300 years BC  
750 (9,500-8,200 years BP) and between 7,500 and 6,200 years BC (9,400-8,100 years BP).  
751 Beyond Brittany, some early *Cerealia*-type occurrences have already been observed as co-  
752 occurring with ruderal plants between 6,400 and 5,800 years BC (8,400-7,800 years BP) in  
753 the northern Pyrenean region by *Galop and Vaquer (2004)* or between 6,600 and 5,800 years  
754 BC (8,600-7,800 years BP) in the Parisian Basin (*Leroyer and Allenet, 2006*). In addition,  
755 occurrences of *Cerealia*-type pollen grains have been reported from many Swiss sites  
756 between 7,750 and 5,800 Cal. BC (*Erny-Rodmann et al., 1997; Lotter, 1999; Tinner et al.,*

757 1999, 2007; Beckmann, 2004; Fig. 15). Taking into account our data and the numerous  
758 references cited above, we underline the great timing coherence of large Poaceae pollen grain  
759 appearances, with sizes usually interpreted as resulting from a cultivated origin. Among the  
760 reservations that are often opposed to these detections (e.g. reliability of dating, long-distance  
761 transport or laboratory contaminations; Behre, 2007), we can consider minimal errors in  
762 carbon datings (see the core stratigraphy) or in laboratory treatments that are identical for all  
763 cores (i.e. Roscanvel “A” core, without any large Poaceae pollen grain). Regarding the long-  
764 distance transport of pollen grains from the eastern areas where cereals were already  
765 cultivated, as already mentioned by Tinner *et al.* (2007), it is surprising that we do not detect  
766 pollen grains from other exotic species with a better pollen dispersion than cereals (e.g.  
767 *Quercus ilex*, *Pistacia*). Moreover, the BB and BD watersheds are too small to receive long-  
768 transported pollen grains from eastern or southern sites. We can thus suggest two hypotheses:

769 1. These atypical large pollen grains are not inherited from cultures and represent a signature  
770 of littoral grasses. Indeed, some coastal Poaceae on the Atlantic coast may have pollen grains  
771 that can reach large sizes (Joly *et al.*, 2007). The size threshold which is considered by  
772 palynologists as a robust identification criteria for the determination of cereal pollen grains,  
773 may be revised again (cf. Joly *et al.*, 2007) in light of the particular pollen sizes of some  
774 regional littoral grasses. Regarding this first hypothesis, it still appears curious not to detect  
775 any significant increase in total Poaceae or Chenopodiaceae when the most relevant peaks of  
776 *Cerealia*-type pollen grains are recorded (Fig. 7b). Furthermore, in the Bay of Roscanvel  
777 records (A and KS-24 cores, Fig. 9b), studied from 9,200 to 5,300 years BP in same  
778 environmental sedimentary context, the total absence of these large pollen grains of Poaceae  
779 before 8,600 years BP implies no peculiarity of size among pollen grains from littoral grasses.

780 2. A discreet proto-agriculture signal would be recorded for the first time during the  
781 Mesolithic in western Brittany. Discussed by the Mesolithic archaeological community, this

782 type of “agriculture” would be characterized by its discretion in the landscape and the absence  
783 of specific hard rock made agricultural tools (*Marchand, 2005*). The work of plants seems  
784 indeed to grown toward the end of the Mesolithic, but regional use-wear analysis on  
785 archeological material suggested that wear traces result from scrapping of wood and soft  
786 plants, with however no traces of cereal plant work (e.g. *Gassin et al., 2013*; Beg an Dorchen,  
787 SW Brittany). In the previous palynological studies mentioned above (Fig. 15), *Cerealia*-type  
788 pollen grain occurrences are always scarce and isolated in space and time (*Visset et al., 2002*).  
789 Our study, conducted on a core taken in the marine coastal domain, enables to record a  
790 temporal BD watershed signal with iterative occurrences of these large pollen grains (8,482;  
791 8,440; 8,395 years BP or 6,532; 6,490; 6,445 years BC) associated with some other cultural  
792 indicators as *Plantago lanceolata* and *Rumex* spp. (Fig. 14). The scarcity of Mesolithic data  
793 on the territory, and the difficulties to identify proto-agriculture evidence, both with pollen or  
794 lithic data, does not allow to discuss the local introduction of this proto-agriculture imprint as  
795 a result from a meridional migration movement (Retzian culture *via* the Loire estuary; *Visset*  
796 *et al., 2002*) or from the main Neolithic cultural in Brittany from a Danubian origin  
797 (*Dubouloz, 2003*; *Gomart et al., 2015*; Fig. 15).

798 In order to progress, future studies must be conducted i) to newly establish the size  
799 variation of the current littoral wild grass pollen grains, ii) to confirm the timing of the first  
800 large pollen grain detection at a broader regional-scale.

801

## 802 **6. Conclusion**

803 Our results allowed characterizing Holocene coastal palaeoenvironments of NW France (Bay  
804 of Brest and Bay of Douarnenez, western Brittany) over two given periods (9,200-8,400 and  
805 6,600-5,300 years BP). Various factors forced coastal environmental changes during the early  
806 to mid-Holocene especially including the relative sea-level rise that modified sedimentation  
807 processes and the post-glacial recolonization of temperate trees. Sedimentological and  
808 palynological analyses carried out in this study allowed us to characterize and specify the  
809 environmental variations that impacted coastal environments of western Brittany. The relative  
810 sea-level rise influenced the sedimentary infilling history of shallow marine environments that  
811 transited from river valleys to oceanic bays. In addition, high resolution studies enabled us to  
812 detect the regional response to more global events arising from the millennial-scale climate  
813 variability in the North Atlantic. Thus, around 8,600 and 6,000 years BP, onsets of two major  
814 abrupt climate events are locally detected by a moisture increase marked by strong  
815 occurrences of *Corylus*, *Alnus*, and *L. machaerophorum* dinocyst taxon. In addition, the  
816 gradual decrease of continental summer temperatures is marked by the withdrawal of  
817 thermophilous species *Ulmus* and *Tilia*. Moreover, during this time period also marked by the  
818 appearance of the neolithisation, *Cerealia*-type pollen grains have been detected in the Bay of  
819 Douarnenez, about 1,500 years before the advent of agriculture commonly accepted. These  
820 local results, while being consistent with other palynological studies conducted on the French  
821 Atlantic coast, must be taken with caution and open the way to further studies so as to confirm  
822 these "pre-domestic" agriculture indices.

## 7. Acknowledgements

823  
824  
825 This study was supported by the French CNRS and is a contribution to the 2015-2016 INSU  
826 project EC2CO-LEFE: « *CAMOMI : Convergences / Approches croisées des signaux*  
827 *MOléculaires et Mlcropaléontologiques pour décrypter les forçages anthropiques et*  
828 *climatiques en milieu côtier (Rade de Brest)* » and the UBO-BQR project : « *PARADE :*  
829 *Signature PALéoenvironnementale des séquences holocènes en RADE de Brest* ». This work  
830 was supported by the «Laboratoire d'Excellence» LabexMER (ANR-10-LABX-19) and co-  
831 funded by a grant from the French government under the program « *Investissements*  
832 *d'Avenir* ». We thank the UMR CNRS 5805 EPOC (Talence) for palynological laboratory  
833 procedures (Muriel Georget), the UMS 2572 LMC14 (Saclay) for carbon dating via Artemis  
834 project fundings, the sedimentology laboratory of the Shom (« *Service Hydrographique et*  
835 *Océanographique de la Marine*») for the VC-08 core taken from the Bay of Douarnenez  
836 (PROTEUS-DUNES cruises; 2012), the laboratory IFREMER-Marine Geosciences  
837 (Plouzané) for the KS-24 core collected in the Bay of Brest (SERABEQ cruises; G. Gregoire  
838 PhD thesis, 2016) and the LEMAR laboratory (« *Laboratoire des Sciences de l'Environnement*  
839 *Marin*»; IUEM, Plouzané) for the A core taken from the Bay of Brest (Défis Golfe de  
840 Gascogne cruise; 2003). Main issues of this project are integrated within the theme  
841 "Dynamics of Human Settlement and Paleoenvironments » of the Zone Atelier Brest Iroise  
842 (ZABrI, INEE-CNRS).

## References

843  
844  
845 Amat, A. E. 1995. Evolución del paisaje durante los últimos 10000 años en las montañas del  
846 Mediterráneo Occidental : ejemplos del Pirineo Oriental y Sierra Nevada. PhD thesis,  
847 University of Barcelona.

848 Augris, C., Érik, H., Joël, R. 1988. Carte des Sédiments Superficiels et Carte Géologique de  
849 La Baie de Douarnenez: Partie Septentrionale. Ifremer.

850 Augris, C., Ménesguen, A., Hamon, D., Blanchet, A., Le Roy, P., Rolet, J., Jouet, G., Véron,  
851 G., Delannoy, H., Drogou, M., Bernard, C., Maillard, X. 2005. Atlas thématique de  
852 l'environnement marin de la Baie de Douarnenez. Ifremer (Ed). pp. 61-72.

853 Ballèvre, M., Bosse, V., Ducassou, C., Pitra, P. 2009. Palaeozoic history of the Armorican  
854 Massif: models for the tectonic evolution of the suture zones. *Comptes Rendus Geoscience*,  
855 341, 174–201.

856 Ballèvre, M., Bosse, V., Dabard, M.-P., Ducassou, C., Fourcade, S., Paquette, J.-L., Peucat,  
857 J.-J., and Pitra, P. 2013. Histoire Géologique Du Massif Armoricaïn: Actualité de La  
858 Recherche. *Bulletin de La Société Géologique et Minéralogique de Bretagne* 500, 5–96.

859 Barbier, D., Visset, L. 1997. “Logné, a Peat Bog of European Ecological Interest in the  
860 Massif Armoricaïn, Western France: Bog Development, Vegetation and Land-Use History.”  
861 *Vegetation History and Archaeobotany* 6, 69–77.

862 Beckmann, M. 2004. Pollenanalytische Untersuchung der Zeit der Jäger und-Sammler und  
863 der ersten Bauern an zwei Lokalitäten des-Zentralen Schweizer Mittellandes: Umwelt und  
864 erste Eingriffe des Menschen in die Vegetation vom Paläolithikum bis zum Jungeneolithikum.  
865 *Dissertationes Botanicae* 390. Berlin: J. Cramer.

866 Behre, K. E. 1981. The interpretation of anthropogenic indicators in pollen diagrams. *Pollen*  
867 *et spores*, 23(2), 225-245.

868 Behre, K.E. 2007. Evidence for Mesolithic agriculture in and around central Europe ?  
869 *Vegetation History and Archaeobotany* 16, 2-3, 203-219.

870 Belleguic, K., Conseil, C., Eveno, T., Lorge, S., Baraer, F. 2012. “Le Changement Climatique  
871 en Bretagne.” Météo France, 85p.

872 Berger, A., Loutre, M. F. 1991. Insolation values for the climate of the last 10 million years.  
873 *Quaternary Science Reviews*, 10(4), 297-317.

874 Beug, H.-J., 1961. Leitfaden der pollenbestimmung. Fisch. Stuttg. 1, 63. 542 pp

875 Beug, H. J. 1965. Pollenanalytische Untersuchungen zur nacheiszeitlichen Geschichte der  
876 mediterranen Art im Gardasee-Gebiet. *Plant Biology* 1, 78, 28-30.

877 Beug, H.J., 2004. Leitfaden der Pollenbestimmung für Mitteleuropa und angrenzende  
878 Gebiete. Verlag Friedrich Pfeil, Munich, 542 p.

879 Blanchet, S., Kayser, O., Marchand G., Yven E. 2006. “Le Mésolithique Moyen En Finistère:  
880 De Nouvelles Datations Pour Le Groupe de Bertheaume.” *Bulletin de La Société*  
881 *Préhistorique Française*, 507–517.

882 Blanchet, S., Forré, P., Fromont, N., Hamon, C., Hamon, G. (2010). Un habitat du  
883 Néolithique ancien à Betton «Pluvignon» (Ille-et-Vilaine). Présentation synthétique et  
884 premiers résultats. *Premiers Néolithiques de l’Ouest. Cultures, réseaux, échanges des*  
885 *premières sociétés néolithiques à leur expansion. Presses Universitaires de France, Rennes,*  
886 *15-40.*

887 Bond, G., Showers, W., Cheseby, M., Lotti, R., Almasi, P., Priore, P., Cullen, H., Hajdas, I.,  
888 Bonani, G. 1997. “A Pervasive Millennial-Scale Cycle in North Atlantic Holocene and  
889 Glacial Climates.” *Science*, 278, 1257–1266.

890 Bond, G., Kromer, B., Beer, J., Muscheler, R., Evans, M.N., Showers, W., Hoffmann, S.,  
891 Lotti-Bond, R., Hajdas, I., and Bonani, G. 2001. “Persistent Solar Influence on North Atlantic  
892 Climate during the Holocene.” *Science*, 294, 2130–2136.

893 Bonnet, S., Guillocheau, F., Brun, J.-P., Van Den Driessche, J., 2000. Large-scale relief  
894 development related to Quaternary tectonic uplift of a Proterozoic-Paleozoic basement: The  
895 Armorican Massif, NW France. *Journal of Quaternary Research*, 105, 19273-19288.

896 Bradbury, J.P, Dean, W.E., Anderson, R.Y. 1993. "Holocene Climatic and Limnologic  
897 History of the North-Central United States as Recorded in the Varved Sediments of Elk Lake,  
898 Minnesota: A Synthesis." *Geological Society of America Special Papers*, 276, 309–328.

899 Bramanti, B., Thomas, M. G., Haak, W., Unterländer, M., Jores, P., Tambets, K., Antanaitis-  
900 Jacobs, I., Haidle, M. N., Jankauskas, R., Kind, C. J., Lueth, F., Terberger, T., Hiller, J.,  
901 Matsumura, S., Forster, P., Burger, J. 2009. Genetic discontinuity between local hunter-  
902 gatherers and central Europe's first farmers. *science*, 326(5949), 137-140.

903 Brewer, S., Cheddadi, R., De Beaulieu, J. L., Reille, M. 2002. The spread of deciduous  
904 *Quercus* throughout Europe since the last glacial period. *Forest Ecology and Management*,  
905 156(1), 27-48.

906 Carcaud, N., Cyprien, A. L., Visset, L. 2000. Marais et vallée de la Loire, mémoire des  
907 paysages depuis dix mille ans. Étude comparative des marais de Distré et Champtocé et de la  
908 vallée de la Loire à Montjean-sur-Loire. *Archives d'Anjou*, 4, 187-215.

909 Cassen, S., Audren, C., Hinguant, S., Lannuzel, G., Marchand, G. 1998. L'habitat Villeneuve-  
910 Saint-Germain du Haut-Mée (Saint-Étienne-en-Coglès, Ille-et-Vilaine). *Bulletin de la Société*  
911 *préhistorique française*, 41-75.

912 Chauris, L., Plusquellec, Y., (coord) 1980. *Carte Geol. France (1/50 000), feuille Brest (274)*.  
913 Ed. B.R.G.M., Orléans.

914 Cupillard, C., Magny, M., Richard, H., Ruffaldi, P., Marguier, S. 1994. Mésolithisation et  
915 néolithisation d'une zone de moyenne montagne (évolution du peuplement et du paysage de la



916 haute vallée du Doubs). Rapport de fin de contrat A.T.P. « Archéologie Métropolitaine »,  
917 Laboratoire de Chrono-Ecologie, 120 p.

918 David, R. 2014. Modélisation de la végétation holocène du Nord-Ouest de la France:  
919 reconstruction de la chronologie et de l'évolution du couvert végétal du Bassin parisien et du  
920 Massif armoricain. Thèse de doctorat. Université Rennes 1.

921 Davis, B.A., Brewer, S., Stevenson, A.C., Guiot, J., 2003. The temperature of Europe during  
922 the Holocene reconstructed from pollen data. *Quaternary Science Reviews*, 22, 1701–1716.

923 Debenay, J. P., Bicchi, E., Goubert, E., Du Châtelet, E. A. 2006. Spatio-temporal distribution  
924 of benthic foraminifera in relation to estuarine dynamics (Vie estuary, Vendée, W France).  
925 *Estuarine, Coastal and Shelf Science*, 67(1), 181-197.

926 Delaine, M., Armynot du Châtelet, E., Bout-Roumazelles, V., Goubert, E., Le Cadre, V.,  
927 Recourt, P., Trentesaux, A., Arthuis, R. 2015. Multiproxy approach for Holocene  
928 paleoenvironmental reconstructions from microorganisms (testate amoebae and foraminifera)  
929 and sediment analyses: The infilling of the Loire Valley in Nantes (France). *The Holocene*,  
930 25(3), 407-420.

931 Delmas, R., Treguer, P., 1983. Evolution saisonnière des nutriments dans un écosystème  
932 eutrophe d'Europe occidentale (la rade de Brest). *Interactions marines et terrestres*.  
933 *Oceanologica Acta*, 6, 345–356.

934 Deser, C., Alexander, M. A., Xie, S. P., Phillips, A. S. 2010. Sea surface temperature  
935 variability: Patterns and mechanisms. *Annual review of marine science*, 2, 115-143.

936 Dubouloz, J. 2003. Datation absolue du premier Néolithique du Bassin parisien: complément  
937 et relecture des données RRBP et VSG. *Bulletin de la Société préhistorique française*, 671-  
938 689.

939 de Vernal, A., Henry, M., Bilodeau, G., 1999. Techniques de préparation et d'analyse en  
940 micropaléontologie. Les Cahiers du GEOTOP, 3, 1-31.

941 de Vernal, A., Hillaire-Marcel, C., Rochon, A., Fréchette, B., Henry, M., Solignac, S.,  
942 Bonnet, S. 2013. Dinocyst-based reconstructions of sea ice cover concentration during the  
943 Holocene in the Arctic Ocean, the northern North Atlantic Ocean and its adjacent seas.  
944 Quaternary Science Reviews, 79, 111-121.

945 Dodge, J. D., Harland, R. 1991. The distribution of planktonic dinoflagellates and their cysts  
946 in the eastern and northeastern Atlantic Ocean. New Phytologist, 118(4), 593-603.

947 Dréano Y., Giovannacci S., Dupont C., Gruet Y., Hoguein R., Ihuel E., Leroy A., Marchand  
948 G., Pailler Y., Sparfel Y., Tresset A. 2007 - Le patrimoine archéologique de l'île Béniguet (Le  
949 Conquet, Finistère) - Bilan des recherches 2000-2007, In Quinze ans d'étude et de recherches  
950 sur la réserve de Béniguet, Bulletin de la Société des Sciences Naturelles de l'Ouest de la  
951 France, nouvelle série, 29, 161-172.

952 Duplessy, J. C. 1978. Isotope studies. Climatic change, 3, 47-67.

953 Erny-Rodmann, C., Gross-kee, E., Haas, J. N., Jacomet, S., Zoller, H. 1997. Früher «human  
954 impact» und Ackerbau im Übergangsbereich Spätmesolithikum-Frühneolithikum im  
955 schweizerischen Mittelland. Jahrbuch der Schweizerischen Gesellschaft für Ur-und  
956 Frühgeschichte, 80, 27-56.

957 Estournès, G., Menier, D., Guillocheau, F., Le Roy, P., Paquet, F., Goubert, E. 2012. The  
958 paleo-Etel River incised valley on the Southern Brittany inner shelf (Atlantic coast, France):  
959 Preservation of Holocene transgression within the remnant of a middle Pleistocene incision.  
960 Marine Geology, 329, 75-92.

961 Faegri, K., Iversen, J., (Eds.) 1989. Textbook of pollen analysis. 4th Edition by Faegri, K.,  
962 Kaland, P.E., Krzywinski, K. John Wiley and Sons, Chichester, 328 p.

963 Fatela, F., Taborda, R., 2002. Confidence limits of species proportions in microfossil  
964 assemblages. *Marine Micropaleontology* 45, 169–174.

965 Fernane, A., Gandouin, E., Penaud, A., Van Vliet-Lanoë, B., Goslin, J., Vidal, M., Delacourt,  
966 C., 2014. Coastal palaeoenvironmental record of the last 7 kyr BP in NW France: Sub-  
967 millennial climatic and anthropic Holocene signals. *The Holocene* 24, 1785–1797.

968 Fernane, A., Penaud, A., Gandouin, E., Goslin, J., Van Vliet-Lanoë, B., & Vidal, M. 2015.  
969 Climate variability and storm impacts as major drivers for human coastal marsh withdrawal  
970 over the Neolithic period (Southern Brittany, NW France). *Palaeogeography,*  
971 *Palaeoclimatology, Palaeoecology*, 435, 136-144.

972 Galop, D., Vaquer, J. 2004. Regards croisés sur les premiers indices de l’anthropisation en  
973 domaine pyrénéen. Néolithisation précoce. Premières traces d’anthropisation du couvert  
974 végétal à partir des données polliniques, 7, 179-194.

975 García-Artola A., Stéphan P., Cearreta A., Kopp R.E., Khan N.S., Horton B.P. 2018.  
976 Holocene sea-level database from the Atlantic coast of Europe. *Quaternary Science Reviews*,  
977 196, 177-192.

978 Gassin, B., Marchand, G., Claud, É., Guéret, C., Philibert, S. 2013. Les lames à coches du  
979 second Mésolithique: des outils dédiés au travail des plantes? *Bulletin de la Société*  
980 *préhistorique française*, 25-46.

981 Giot, P. R., L'Helgouach, J., Monnier, J. L. 1998. *Préhistoire de la Bretagne*. Ouest-France.  
982 588 p.

983 Gomart, L., Hachem, L., Hamon, C., Giligny, F., Ilett, M. 2015. Household integration in  
984 Neolithic villages: A new model for the Linear Pottery Culture in west-central Europe.  
985 *Journal of Anthropological archaeology*, 40, 230-249.

986 Gooday, A. J. 2003. Benthic foraminifera (Protista) as tools in deep-water  
987 palaeoceanography: environmental influences on faunal characteristics. *Advances in marine*  
988 *biology*, 46, 1-90.

989 Goslin, J., Vliet-Lanoë, B. V., Stéphan, P., Delacourt, C., Fernane, A., Gandouin, E., Hénaff,  
990 A., Penaud, A., Suanez, S. 2013. Holocene relative sea-level changes in western Brittany  
991 (France) between 7600 and 4000 cal. BP: Reconstitution from basal-peat deposits.  
992 *Géomorphologie: relief, processus, environnement*, 19(4), 425-444.

993 Goslin, J., 2014. L'évolution du niveau marin relatif le long des côtes du Finistère (Bretagne,  
994 France) de 8000 BP à l'actuel: entre dynamiques régionales et réponses locales. PhD Thesis,  
995 IUEM, Brest University, 14 February 2014, pp. 355.

996 Goslin, J., van Vliet Lanoë, B., Spada, G., Bradley, S., Tarasov, L., Neill, S., Suanez, S.,  
997 2015. A new Holocene relative sea-level curve for western Brittany (France): Insights on  
998 isostatic dynamics along the Atlantic coasts of north-western Europe. *Quaternary Science*  
999 *Reviews*, 129, 341–365.

1000 Gouletquer, P., Kayser, O., Le Goffic, M., & Marchand, G. 1994. Approche géographique du  
1001 Mésolithique de la Bretagne. Le Tardiglaciaire en Europe du nordouest, Actes du 119e  
1002 congrès national des Sociétés historiques et scientifiques, Amiens, 279-292.

1003 Gouletquer, P., Kayser, O., Le Goffic, M., Léopold, P., Marchand, G., & Moullec, J. M. 1996.  
1004 Où sont passés les Mésolithiques côtiers bretons? Bilan 1985-1995 des prospections de  
1005 surface dans le Finistère. *Revue archéologique de l'Ouest*, 13(1), 5-30.

1006 Gregoire, G., Ehrhold, A., Le Roy, P., Jouet, G., Garlan, T., 2016. Modern morpho-  
1007 sedimentological patterns in a tide-dominated estuary system: the Bay of Brest (west  
1008 Brittany, France). *Journal of Maps*, 12, 1152-1159.

1009 Gregoire, G., Le Roy, P., Ehrhold, A., Jouet, G., Garlan, T. 2017. Control factors of Holocene  
1010 sedimentary infilling in a semi-closed tidal estuarine-like system: the bay of Brest (France).  
1011 *Marine Geology*, 385, 84-100.

1012 Guenet, P. 1995. Analyse palynologique du sondage du Petit Castelou. In J. Guilaine  
1013 (dir.), *Temps et espace dans le bassin de l'Aude du Néolithique à l'Age du Fer*. Centre  
1014 d'Anthropologie, Toulouse, 334-340.

1015 Guéret, C. 2013. Character and variability of Early Mesolithic toolkits in Belgium and  
1016 Northern France: the contribution of a functional approach. In « *Palethnologie du  
1017 Mésolithique: recherches sur les habitats de plein air entre Loire et Neckar/Mesolithic  
1018 Palethnography* ». Actes de la table ronde internationale de Paris. Société préhistorique  
1019 française Paris, 147-167.

1020 Guéret, C., Gassin, B., Jacquier, J., Marchand, G. 2014. Traces of plant working in the  
1021 Mesolithic shell midden of Beg-an-Dorchenn (Plomeur, France). *Mesolithic Miscellany*,  
1022 22(3), 3-15.

1023 Guilcher, A. 1948. *Le relief de la Bretagne méridionale de la baie de Douarnenez à la Vilaine*.  
1024 PhD. Thèse Paris, H. Potier (éd.), La Roche-sur-Yon, 682 p.

1025 Haak, W., Balanovsky, O., Sanchez, J. J., Koshel, S., Zaporozhchenko, V., Adler, C. J., Der  
1026 Sarkissian, C.S.I., Brandt, G., Scharwtz, C., Nicklisch, N., Dresely, V., Fritsch, B.,  
1027 Balanovska, E. 2010. Ancient DNA from European early neolithic farmers reveals their near  
1028 eastern affinities. *PLoS biology*, 8(11), e1000536.

- 1029 Hallegouët, B. 1989. La presqu'île de Crozon: évolution géomorphologique. *Historien-*  
1030 *Géographe*, 318, 141-148.
- 1031 Hallegouët B., Lozac'h G., Vigouroux F. 1994. Formation de la Rade de Brest. *In Corlay, J.-*  
1032 *P., (coord.) Atlas permanent de la Mer et du Littoral n°1*. Université de Nantes. CNRS-URA-  
1033 904/EDITMAR. p. 21.
- 1034 Hammarlund, D., Björck, S., Buchardt, B., & Thomsen, C. T. 2005. Limnic responses to  
1035 increased effective humidity during the 8200 cal. yr BP cooling event in southern Sweden.  
1036 *Journal of Paleolimnology*, 34(4), 471-480.
- 1037 Hamon, G. 2008. Productions céramiques du Néolithique armoricain. *Bulletin-Société*  
1038 *d'archéologie et d'histoire du Pays de Lorient*, 37, 21-32.
- 1039 Hirschberger, F., Pauvret, R. B. 1968. Les fonds sous-marins de l'Iroise et de la Baie de  
1040 Douarnenez (Finistère). Reconstitution d'un réseau hydrographique immergé. *Norois*, 58(1),  
1041 213-225.
- 1042 Huntley, B. 1993. Rapid early-Holocene migration and high abundance of hazel (*Corylus*  
1043 *avellana* L.): alternative hypotheses. In *Climate change and human impact on the landscape*.  
1044 Springer Netherlands, 205-215.
- 1045 Jalut, G., Vernet, J. L. 1989. La végétation du Pays de Sault et de ses marges depuis 15000  
1046 ans: réinterprétation des données palynologiques et apports de l'anthracologie. *Pays de Sault,*  
1047 *espaces, peuplement, populations*. CNRS, Toulouse, 23-41.
- 1048 Jiang, H., Muscheler, R., Björck, S., Seidenkrantz, M. S., Olsen, J., Sha, L., Sjolte, J.,  
1049 Eiriksson, J., Ran, L., Knudsen, K.L, Knudsen, M. F. 2015. Solar forcing of Holocene  
1050 summer sea-surface temperatures in the northern North Atlantic. *Geology*, 43(3), 203-206.

- 1051 Joly, C., Visset, L. 2005. Nouveaux éléments d'anthropisation sur le littoral vendéen dès la fin  
1052 du Mésolithique. *Comptes Rendus Palevol*, 4(3), 285-293.
- 1053 Joly, C., Barillé, L., Barreau, M., Mancheron, A., Visset, L., 2007. Grain and annulus  
1054 diameter as criteria for distinguishing pollen grains of cereals from wild grasses. *Rev.*  
1055 *Palaeobot. Palynol.* 146, 221–233.
- 1056 Joly, C., Visset, L. 2009. Evolution of vegetation landscapes since the Late Mesolithic on the  
1057 French West Atlantic coast. *Review of Palaeobotany and Palynology*, 154(1), 124-179.
- 1058 Jorissen, F.J., Fontanier, C., Thomas, E. 2007. Chapter seven paleoceanographical proxies  
1059 based on deep-sea benthic foraminiferal assemblage characteristics. *Developments in Marine*  
1060 *Geology*, 1, 263-325.
- 1061 Jouet, G., Augris, C., Hallegouët, B., Le Roy, P., Rolet, J. 2003. La vallée d'Ys: un  
1062 paléoreseau hydrographique immergé en baie de Douarnenez (Finistère, France). *Comptes*  
1063 *Rendus Geoscience*, 335(5), 487-494.
- 1064 Kirleis, W., Kloß, S., Kroll, H., Müller, J. 2012. Crop growing and gathering in the northern  
1065 German Neolithic: a review supplemented by new results. *Vegetation history and*  
1066 *archaeobotany*, 21(3), 221-242.
- 1067 Knight, J.R., Folland, C.K., Scaife, A.A., 2006. Climate impacts of the Atlantic multidecadal  
1068 oscillation. *Geophysical Research Letters*, 33(17).
- 1069 Lambert, C., Vidal, M., Penaud, A., Combourieu-Nebout, N., Lebreton, V., Ragueneau, O.,  
1070 Gregoire, G., 2017. Modern palynological record in the Bay of Brest (NW France): signal  
1071 calibration for palaeo-reconstructions. *Review of Palaeobotany and Palynology* 244, 13-25.

1072 Lambert, C., Penaud, A., Vidal, M., Klouch, K., Gregoire, G., Ehrhold, A., Eynaud, F.,  
1073 Schmidt, S., Ragueneau, O., Siano, R. 2018. Human-induced river runoff overlapping natural  
1074 climate variability over the last 150 years: Palynological evidence (Bay of Brest, NW France).  
1075 *Global and Planetary Change*, 160, 109-122.

1076 Lefort, J. P. 1973. La "zonale" Biscaye-Labrador: mise en évidence de cisaillements dextres  
1077 antérieurs à l'ouverture de l'Atlantique Nord. *Marine Geology*, 14(5), 33-38.

1078 Legigan, P., Marambat, L. 1993. Âge de la formation d'une lagune landaise : premières  
1079 données palynologiques et radiométriques. *Bull. Soc. De Bordeaux*, 118, 432, 433-443.

1080 Le Roy, P., Jouet, G., 2005. Remplissage sédimentaire meuble. In : Augris, C., Ménesguen,  
1081 A., Hamon, D., Blanchet, A., Le Roy, P., Rolet, J., Jouet, G., Véron, G., Delannoy, H.,  
1082 Drogou, M., Bernard, C., Maillard, X., 2005. Atlas thématique de l'environnement marin de  
1083 la Baie de Douarnenez. Ifremer (Ed), 61-72.

1084 Leroyer, C., Mordant, D., Lanchon, Y. 2004. L'anthropisation du Bassin parisien du VIIe au  
1085 IVe millénaire d'après les analyses polliniques de fonds de vallées: mise en évidence  
1086 d'activités agro-pastorales très précoces. Néolithisation précoce. Première trace  
1087 d'anthropisation du couvert végétal à partir des données polliniques, 11-27.

1088 Leroyer, C., Allenet, G. 2006. L'anthropisation du paysage végétal d'après les données  
1089 polliniques: l'exemple des fonds de vallées du Bassin parisien. *L'érosion entre Société,*  
1090 *Climat et Paléoenvironnement. Actes de la Table Ronde en l'honneur de René Neboit-*  
1091 *Guilhot. Coll.«Nature et Société, 3, 63-72.*

1092 Lotter, A. F. 1999. Late-glacial and Holocene vegetation history and dynamics as shown by  
1093 pollen and plant macrofossil analyses in annually laminated sediments from Soppensee,  
1094 central Switzerland. *Vegetation History and Archaeobotany*, 8(3), 165-184.



- 1095 Mangerud, J., Bondevik, S., Gulliksen, S., Hufthammer, A. K., Høisæter, T. 2006. Marine 14  
1096 C reservoir ages for 19th century whales and molluscs from the North Atlantic. *Quaternary*  
1097 *Science Reviews*, 25(23), 3228-3245.
- 1098 Marchand, G. 2005. Le Mésolithique final en Bretagne: une combinaison des faits  
1099 archéologiques. *Mémoires de la Société préhistorique française*, 36, 67-86.
- 1100 Marchand, G., Paillet, Y., Tournay, G. 2006. Carrément à l'Ouest! Indices du Villeneuve-  
1101 Saint-Germain au centre de la Bretagne (le Dillien à Cléguérec et Bellevue à Neulliac;  
1102 Morbihan). *Bulletin de la Société préhistorique française*, 519-533.
- 1103 Marchand, G. 2007. Neolithic fragrances: Mesolithic-Neolithic interactions in western France.  
1104 In *Proceedings-British Academy* (Vol. 144, p. 225). Oxford University Press Inc.
- 1105 Marchand, G. 2014. Préhistoire atlantique: Fonctionnement et évolution des sociétés du  
1106 Paléolithique au Néolithique. Ed. Errance. 519 p.
- 1107 Marcigny, C., Ghesquiere, E., Juhel, L., Charraud, F. 2010. Entre Néolithique ancien et  
1108 Néolithique moyen en Normandie et dans les îles anglo-normandes. *Parcours chronologique.*  
1109 *Premiers Néolithiques de l'Ouest. Cultures, réseaux, échanges des premières sociétés*  
1110 *néolithiques à leur expansion*, 117-62.
- 1111 Marguerie, D. 1991. Confrontation des données polliniques et anthracologiques  
1112 (Défrichement du milieu forestier et développement de la lande régressive à partir du  
1113 Néolithique en Armorique). *Revue d'Archéométrie*, 15(1), 75-82.
- 1114 Marret, F., Zonneveld, K. A. 2003. Atlas of modern organic-walled dinoflagellate cyst  
1115 distribution. *Review of Palaeobotany and Palynology*, 125(1), 1-200.

1116 Mayewski, P. A., Meeker, L. D., Twickler, M. S., Whitlow, S., Yang, Q., Lyons, W. B., &  
1117 Prentice, M. 1997. Major features and forcing of high-latitude northern hemisphere  
1118 atmospheric circulation using a 110,000-year-long glaciochemical series. *Journal of*  
1119 *Geophysical Research: Oceans*, 102(C12), 26345-26366.

1120 Mayewski, P. A., Rohling, E. E., Stager, J. C., Karlén, W., Maasch, K. A., Meeker, L. D.,  
1121 Meyerson, E.A., Gasse, F., van Kreveld, S., Holmgren, K., Lee-Thorpe, J., Rosqvist, G.,  
1122 Rack, F., Staubwasser, M., Schneider, R.R., Steig, E.J. 2004. Holocene climate variability.  
1123 *Quaternary research*, 62(3), 243-255.

1124 McCarthy, G.D., Haigh, I.D., Hirschi, J.J.-M., Grist, J.P., Smeed, D.A., 2015. Ocean impact  
1125 on decadal Atlantic climate variability revealed by sea-level observations. *Nature* 521, 508–  
1126 510.

1127 McClatchie, M., Bogaard, A., Colledge, S., Whitehouse, N. J., Schulting, R. J., Barratt, P.,  
1128 McLaughlin, T. R. 2014. Neolithic farming in north-western Europe: archaeobotanical  
1129 evidence from Ireland. *Journal of Archaeological Science*, 51, 206-215.

1130 Meeker, L. D., Mayewski, P. A. 2002. A 1400-year high-resolution record of atmospheric  
1131 circulation over the North Atlantic and Asia. *The Holocene*, 12(3), 257-266.

1132 Mélou, M., Plusquellec, Y. 1974. “Carte Géologique de La France a1/50000, Feuille de  
1133 Douarnenez, No. 309.” BRGM, Brest.

1134 Mertens, K.N., Verhoeven, K., Verleye, T., Louwye, S., Amorim, A., Ribeiro, S., Deaf, A.S.,  
1135 Harding, I.C., De Schepper, S., González, C., Kodrans-Nsiah, M., De Vernal, A., Henry, M.,  
1136 Radi, T., Dybkjaer, K., Poulsen, N.E., Feist-Burkhardt, S., Chitolie, J., Heilmann-Clausen, C.,  
1137 Londeix, L., Turon, J-L., Marret, F., Matthiessen, J., McCarthy, F.M.G., Prasad, V.,  
1138 Pospelova, V., Kyffin Hughes, J.E., Riding, J.B., Rochon, A., Sangiorgi, F., Welters, N.,

- 1139 Sinclair, N., Thun, C., Soliman, A., Van Nieuwenhove, N., Vink, A., Young, M. 2009.  
1140 Determining the absolute abundance of dinoflagellate cysts in recent marine sediments: the  
1141 Lycopodium marker-grain method put to the test. *Rev. Palaeobot. Palynol.* 157, 238–252.
- 1142 Mojtahid, M., Jorissen, F. J., Garcia, J., Schiebel, R., Michel, E., Eynaud, F., Gillet, H.,  
1143 Cremer, M., Diz Ferreiro, P., Siccha, M., Howa, H. 2013. High resolution Holocene record in  
1144 the southeastern Bay of Biscay: Global versus regional climate signals. *Palaeogeography,*  
1145 *Palaeoclimatology, Palaeoecology*, 377, 28-44.
- 1146 Monbet, Y., Bassoulet, P., 1989. Bilan des connaissances océanographiques en rade de Brest.  
1147 Rapport CEA/IPSN, code DERO/EL 89-23. IFREMER-DEL-BP 70-29280 Plouzane, France,  
1148 106 pp.
- 1149 Moore, P.D., Webb, J.A., Collinson, M.E., 1991. Pollen analysis. 2<sup>nd</sup> Edition. Blackwell  
1150 Scientific Publications, Oxford, 216 pp.
- 1151 Morzadec-Kerfourn, M. T. 1974. Variations de la ligne de rivage armoricaine au Quaternaire:  
1152 analyses polliniques de dépôts organiques littoraux. PhD, Université de Rennes, Institut de  
1153 géologie.
- 1154 Morzadec-Kerfourn, M.T., 1976. La signification écologique des dinoflagellés et leur intérêt  
1155 pour l'étude des variations du niveau marin. *Rev. Micropaléontologie* 18, 229–235.
- 1156 Morzadec-Kerfourn, M.-T., 1977. Les kystes de dinoflagellés dans les sédiments récents le  
1157 long des côtes Bretonnes. *Revue de Micropaléontologie*, 20, 157–166.
- 1158 Morzadec-Kerfourn, M.T., 1979. Les kystes de Dinoflagellés. *Géologie Méditerranéenne* 6,  
1159 221–246.

- 1160 Mudie, P.J., Harland, R., Matthiessen, J., & de Vernal, A. 2001. Marine dinoflagellate cysts  
1161 and high latitude Quaternary paleoenvironmental reconstructions: an introduction. *Journal of*  
1162 *Quaternary Science*, 16(7), 595-602.
- 1163 Musset, R. 1934. La formation du réseau hydrographique de la Bretagne occidentale. *Annales*  
1164 *de Géographie*. Colin A. (Ed.), 43, 246, 561-578
- 1165 Naughton, F., Bourillet, J. F., Sánchez Goñi, M. F., Turon, J. L., Jouanneau, J. M. 2007.  
1166 Long-term and millennial-scale climate variability in northwestern France during the last  
1167 8850 years. *The Holocene*, 17(7), 939-953.
- 1168 Nesje, A., Matthews, J. A., Dahl, S. O., Berrisford, M. S., Andersson, C. 2001. Holocene  
1169 glacier fluctuations of Flatebreen and winter-precipitation changes in the Jostedalsbreen  
1170 region, western Norway, based on glaciolacustrine sediment records. *The Holocene*, 11(3),  
1171 267-280.
- 1172 Nielsen, A. B. 2003. Pollen Based Quantitative Estimation of Land Cover: Relationships  
1173 Between Pollen Sedimentation in Lakes and Land Cover as Seen on Historical Maps in  
1174 Denmark AD 1800: PhD, GEUS, Geological Survey of Denmark and Greenland.
- 1175 O'Brien, S.R., Mayewski, P.A., Meeker, L.D., Meese, D.A., Twickler, M.S., & Whitlow, S.I.  
1176 1995. Complexity of Holocene climate as reconstructed from a Greenland ice core. *Science*,  
1177 270(5244), 1962-1964.
- 1178 Ouguerram, A., Visset, L. 2001. Paysages et interactions homme/milieu dans la moyenne  
1179 vallée de l'Erdre du Néolithique aux Époques actuelles: Étude pollinique des marais de Lisle.  
1180 *Annales de Bretagne et des pays de l'Ouest*. Université de Haute-Bretagne, 108(1), 129-146.
- 1181 Pailler, Y., Stéphan, P., Gandois, H., Nicolas, C., Sparfel, Y., Tresset, A., Donnart, K.,  
1182 Fichaut, B., Suanez, S., Dupont, C., Le Clézio, L., Marcoux, N., Pineau, A., Salanova, L.,

- 1183 Sellami, F., Debue, K., Josselin, J., Dietxch-Sellami, M.F. 2011. Évolution des paysages et  
1184 occupation humaine en mer d'Iroise (Finistère, Bretagne) du Néolithique à l'Âge du Bronze.  
1185 *Norois. Environnement, aménagement, société*, (220), 39-68.
- 1186 Pailler, Y., Stéphan, P., Gandois, H., Nicolas, C., Sparfel, Y., Tresset, A., Donnart, K.,  
1187 Dréano, Y., Fichaut, B., Suanez, S., Dupont, C., Audouard, L., Marcoux, N., Mougne, C.,  
1188 Salanova, L., Sellami, F., Dietsch-Sellami, M.-F. 2014. Landscape evolution and human  
1189 settlement in the Iroise Sea (Brittany, France) during the Neolithic and Bronze Age.  
1190 *Proceedings of the Prehistoric Society* (80), 105-139. Cambridge University Press.
- 1191
- 1192 Perez-Belmonte, L. 2008. Caractérisation environnementale, morphosédimentaire et  
1193 stratigraphique du Golfe du Morbihan pendant l'Holocène terminal: Implications évolutives.  
1194 PhD, Université de Bretagne Sud.
- 1195 Puertas, O. 1999. Premiers indices polliniques de néolithisation dans la plaine littorale de  
1196 Montpellier (Hérault, France). *Bulletin de la Société préhistorique française*, 15-20.
- 1197 Redois, F. 1996. Les foraminifères benthiques actuels bioindicateurs du milieu marin  
1198 exemples du plateau continental sénégalais et de l'estran du golfe du Morbihan (France). PhD,  
1199 Université d'Angers.
- 1200 Reille, M., 1995. Pollen et spores d'Europe et d'Afrique du Nord: supplement 1. Laboratoire  
1201 de Botanique Historique et Palynologie, Marseille, 327 pp.
- 1202 Reimer, P. J., Bard, E., Bayliss, A., Beck, J. W., Blackwell, P. G., Ramsey, C. B., Buck, C.E.,  
1203 Cheng, H., Edwards, R.L., Friedrich, M., Grootes, P.M., Guilderson, T.P., Haflidason, H.,  
1204 Hajdas, I., Hatté, C., Heaton, T.J., Hoffmann, D.L., Hogg, A.G., Hughen, K.A., Kaiser, K.F.,  
1205 Kromer, B., Manning, S.W., Niu, M., Reimer, R.W., Richards, D.A., Scott, E.M., Southon,

1206 J.R., Staff, R.A., Turney, C.S.M., van der Plicht, J.. 2013. IntCal13 and Marine13 radiocarbon  
1207 age calibration curves 0–50,000 years cal BP. *Radiocarbon*, 55(4), 1869-1887.

1208 Rochon, A., de Vernal, A. 1994. Palynomorph distribution in recent sediments from the  
1209 Labrador Sea. *Canadian Journal of Earth Sciences*, 31(1), 115-127.

1210 Rochon, A., de Vernal, A. de, Turon, J.-L., Matthiessen, J., Head, M.J., 1999. Distribution of  
1211 recent dinoflagellate cysts in surface sediments from the North Atlantic Ocean and adjacent  
1212 seas in relation to sea-surface parameters. *Am. Assoc. Stratigr. Palynol. Contrib. Ser. 35*, 1–  
1213 146.

1214 Rossi, V., Horton, B. P., Corbett, D. R., Leorri, E., Perez-Belmonte, L., Douglas, B. C. 2011.  
1215 The application of foraminifera to reconstruct the rate of 20th century sea level rise, Morbihan  
1216 Golfe, Brittany, France. *Quaternary Research*, 75(1), 24-35.

1217 Ruddiman, W. F., McIntyre, A. 1981. The North Atlantic Ocean during the last deglaciation.  
1218 *Palaeogeography, Palaeoclimatology, Palaeoecology*, 35, 145-214.

1219 Ruffaldi, P. 1999. Premières traces polliniques de néolithisation des zones de basse altitude de  
1220 Lorraine (France) [First pollen evidences of an neolithic presence in low altitude areas,  
1221 Lorraine (France)]. *Quaternaire*, 10(4), 263-270.

1222 Ruprich-Robert, Y., Cassou, C., 2015. Combined influences of seasonal East Atlantic Pattern  
1223 and North Atlantic Oscillation to excite Atlantic multidecadal variability in a climate model.  
1224 *Climate Dynamics*, 44(1-2), 229–253.

1225 Sampietro, M. L., Lao, O., Caramelli, D., Lari, M., Pou, R., Marti, M., Bertranpetit, J.,  
1226 Lalueza-Fox, C. 2007. Palaeogenetic evidence supports a dual model of Neolithic spreading  
1227 into Europe. *Proceedings of the Royal Society of London B: Biological Sciences*, 274(1622),  
1228 2161-2167.

- 1229 Schulting, R. J., Richards, M. P. 2001. Dating women and becoming farmers: new  
1230 palaeodietary and AMS dating evidence from the Breton Mesolithic cemeteries of Tévéc and  
1231 Hoëdic. *Journal of Anthropological Archaeology*, 20(3), 314-344.
- 1232 Skoglund, P., Malmström, H., Raghavan, M., Storå, J., Hall, P., Willerslev, E., Gilbert,  
1233 M.T.P., Götherström, A., Jakobsson, M. 2012. Origins and genetic legacy of Neolithic  
1234 farmers and hunter-gatherers in Europe. *Science*, 336(6080), 466-469.
- 1235 Steinhilber, F., Beer, J., Fröhlich, C. 2009. Total solar irradiance during the Holocene.  
1236 *Geophysical Research Letters*, 36(19).
- 1237 Stéphan, P. 2008. Les flèches de galets de Bretagne: morphodynamiques passée, présente et  
1238 prévisible. Thèse de Doctorat. Université de Bretagne Occidentale.
- 1239 Stéphan, P., Goslin, J. 2014. Évolution du niveau marin relatif à l'Holocène le long des côtes  
1240 françaises de l'Atlantique et de la Manche: réactualisation des données par la méthode des  
1241 «sea-level index points». *Quaternaire : Revue de l'Association française pour l'étude du*  
1242 *Quaternaire*, 25(4), 295-312.
- 1243 Stéphan, P., Goslin, J., Pailler, Y., Manceau, R., Suanez, S., Vliet-Lanoë, V., Hénaff, A.,  
1244 Delacourt, C. 2015. Holocene salt-marsh sedimentary infilling and relative sea-level changes  
1245 in West Brittany (France) using foraminifera-based transfer functions. *Boreas*, 44(1), 153-  
1246 177.
- 1247 Stuiver, M., Reimer, P. J. 1993. Extended 14C data base and revised CALIB 3.0 14C age  
1248 calibration program. *Radiocarbon*, 35(1), 215-230.
- 1249 Tinevez, J. Y., Hamon, N., Querré, G., Marchand, G., Pailler, Y., Darboux, J. R., Donnart, K.,  
1250 Marcoux, N., Pustoc'h, F., Quesnel, L., Oberlin, C. 2015. Les vestiges d'habitat du

- 1251 Néolithique ancien de Quimper, Kervouyec (Finistère). Bulletin de la Société préhistorique  
1252 française, 112(2), 269-316.
- 1253 Tinner, W., Hubschmid, P., Wehrli, M., Ammann, B., Conedera, M. 1999. Long-term forest  
1254 fire ecology and dynamics in southern Switzerland. *Journal of Ecology*, 87(2), 273-289.
- 1255 Tinner, W., Lotter, A. F. 2001. Central European vegetation response to abrupt climate  
1256 change at 8.2 ka. *Geology*, 29(6), 551-554.
- 1257 Tinner, W., Nielsen, E. H., Lotter, A. F. 2007. Mesolithic agriculture in Switzerland? A  
1258 critical review of the evidence. *Quaternary Science Reviews*, 26(9-10), 1416-1431.
- 1259 Tréguer, P., Goberville, E., Barrier, N., L'Helguen, S., Morin, P., Bozec, Y., Rimmelin-  
1260 Maury, P., Czamanski, M., Grossteffan, E., Cariou, T., Répécaud, M., Quémener, L. 2014.  
1261 Large and local-scale influences on physical and chemical characteristics of coastal waters of  
1262 Western Europe during winter. *Journal of Marine Systems*, 139, 79–90.
- 1263 Triat-Laval, H. 1978: Contribution pollenanalytique à l'histoire tardi-et postglaciaire de la  
1264 végétation de la basse vallée du Rhône. Thèse de doctorat de l'Université d'Aix-Marseille III,  
1265 343 pp.
- 1266 Troadec, P., Le Goff, R., 1997. Etat des lieux et des milieux de la rade de Brest et de son  
1267 bassin versant. Phase Préliminaire du Contrat Baie Rade Brest. Edition Communauté Urbaine  
1268 de Brest, 335 pp.
- 1269 Visset, L. 1979. Recherches palynologiques sur la végétation pleistocene et holocene de  
1270 quelques sites du district phytogéographique de basse-loire. PhD, Université de Nantes.
- 1271 Visset, L., L'Helgouac'h, J., Bernard, J. 1996. La tourbière submergée de la pointe de  
1272 Kerpenhir à Locmariaquer (Morbihan). Etude environnementale et mise en évidence de



- 1273 déforestations et de pratiques agricoles néolithiques. *Revue archéologique de l'Ouest*, 13(1),  
1274 79-87.
- 1275 Visset, L., Hauray, G., Charrieau, L., Rouzeau, N. 2001. Paléoenvironnement urbain: histoire  
1276 du comblement des vallées de la métropole nantaise, du Tardiglaciaire à la fin de l'Holocène.  
1277 In *Annales de Bretagne et des pays de l'Ouest*, Université de Haute-Bretagne, 108(1), 147-  
1278 165.
- 1279 Visset, L., Cyprien, A. L., Carcaud, N., Ouguerram, A., Barbier, D., Bernard, J. 2002. Les  
1280 prémices d'une agriculture diversifiée à la fin du Mésolithique dans le Val de Loire (Loire  
1281 armoricaine, France). *Comptes Rendus Palevol*, 1(1), 51-58.
- 1282 Visset, L., Bernard, J. 2006. Evolution du littoral et du paysage, de la presqu'île de Rhuy à la  
1283 rivière d'Étel (Massif armoricain–France), du Néolithique au Moyen Âge. *ArchéoSciences*.  
1284 *Revue d'archéométrie*, (30), 143-156.
- 1285 von Cramon-Taubadel, N., Pinhasi, R. 2011. Craniometric data support a mosaic model of  
1286 demic and cultural Neolithic diffusion to outlying regions of Europe. *Proceedings of the*  
1287 *Royal Society of London B: Biological Sciences*.
- 1288 Wanner, H., Solomina, O., Grosjean, M., Ritz, S. P., & Jetel, M. 2011. Structure and origin of  
1289 Holocene cold events. *Quaternary Science Reviews*, 30(21), 3109-3123.
- 1290 Willcox, G. 2005. The distribution, natural habitats and availability of wild cereals in relation  
1291 to their domestication in the Near East: multiple events, multiple centres. *Vegetation History*  
1292 *and Archaeobotany*, 14(4), 534-541.
- 1293 Ziegler, P.A., 1992. European Cenozoic rift system. *Tectonophysics* 208, 91–111.

1294 Zonneveld, K.A., Marret, F., Versteegh, G.J., Bogus, K., Bonnet, S., Bouimetarhan, I.,  
1295 Crouch, E., de Vernal, A., Elshanawany, R., Edwards, L., Esper, O., Forke, S., Grosfeld, K.,  
1296 Henry, M., Holzwarth, U., Kielt, J-F., Kim, S-Y., Ladouceur, S., Ledu, D., Chen, L.,  
1297 Limoges, A., Londeix, L., Lu, S-H., Mahmoud, M.S., Marino, G., Matouka, K., Matthiessen,  
1298 J., Mildenthal, D.C., Mudie, P., Neil, H.L., Pospelova, V., Qi, Y., Radi, T., Richerol, T.,  
1299 Rochon, A., Sangiorgi, F., Solignac, S., Turon, J-L., Verleye, T., Wang, Y., Wang, Z., Young,  
1300 M. 2013. Atlas of modern dinoflagellate cyst distribution based on 2405 data points. Rev.  
1301 Palaeobot. Palynol. 191, 1–197.

1302

### 1303 **Figure caption**

1304

1305 Figure 1: a) Location of study sites in North Western France; location of sediment cores on  
1306 the bathymetric maps of the (b) Bay of Douarnenez (black star) and of the (c) Bay of Brest  
1307 (white stars).

1308 Figure 2: Schematic scenario of the Bay of Douarnenez sediment infilling (after Le Roy and  
1309 Jouet, 2005). Four sketches related to the sedimentary units defined from seismic and  
1310 sedimentological analyses (cf details *in* Le Roy and Jouet, 2005).

1311 Figure 3: a) Pictures and b) XR radiography of the VC-08 core. The red strips represent the  
1312 sampled core portion to perform palynological analyzes.

1313 Figure 4: Sedimentological log of the VC-08 core (b), grain size evolution and magnetic  
1314 susceptibility along the core (a). For the different sedimentary units (identified by color  
1315 strips), a graph representing the grain percentages distribution by size was added. <sup>14</sup>C dates  
1316 are represented by red stars on the log.

1317 Figure 5: Cores of the Bay of Brest, “A” and KS-24, and their location on a MNT of the Bay  
1318 of Roscanvel with their bathymetric position (c). Sedimentological logs, photographs and X-  
1319 ray radiography for the “A” (a) and KS-24 cores (b). The <sup>14</sup>C dates are represented on the logs  
1320 by red stars. The red strips represent the sampled core portion to perform palynological  
1321 analyzes.

1322 Figure 6: a) VC-08 (Bay of Douarnenez) and b) “A” core (Bay of Brest) age models with their  
1323 sedimentological logs., linear regression lines (in black) and sedimentation rates in cm/yr.

1324 Figure 7: Graphs against depths with major taxa (greater than 2%) of dinocysts (a) and pollen  
1325 (b) along the VC-08 core, Bay of Douarnenez. The <sup>14</sup>C dates are represented by red stars. The  
1326 dotted lines represent the pollen concentration peaks.

1327 Figure 8: Diagram depicted in ages, from the VC-08 core, grouping together data from  
1328 palynological counting (Pollen, dinocyst and spore concentrations, percentages of trees,  
1329 *Corylus*, *Quercus*, Poaceae, Brassicaceae, *Rumex*, *Cerealia*, the dinocyst *L.machaerophorum*  
1330 and the total Pollen / dinocysts ratio), and the magnetic susceptibility, with respect to  
1331 sedimentary units defined in Figure 4.

1332 Figure 9: Diagram in depth grouping the major taxa (greater than 2%) of dinocysts (a) and  
1333 pollen (b) for the “A” and KS-24 cores, both taken from the Bay of Roscanvel and plotted one  
1334 above the other according to the time periods covered by the two sequences. The <sup>14</sup>C dates are  
1335 represented by red stars. For the “A” core, the most significant minor pollen taxa (greater than  
1336 1%) were also reported. The dotted lines represent the pollen concentration peaks.

1337 Figure 10: Major benthic foraminiferal taxa data plotted against depths (greater than 2%) in  
1338 the “A” and KS-24 cores. <sup>14</sup>C dates are represented by red stars. *Ammonia spp*, *Cibicides spp*,  
1339 *P. mediterraneensis*, Epiphytic species, *Lagena spp* and Miliolidae are represented in  
1340 percentages according to a main sum excluding the *Elphidium* species, major taxa that greatly

1341 tainted the individual signal of each one. The isotopic data measured on shells of *E.*  
1342 *aculeatum* species are added to the graph.

1343 Figure 11: Mean palynological (pollen and dinocysts) and micropalaeontological (benthic  
1344 foraminifera) data for the “A” and KS-24 cores represented in pie charts (a). Diagrams  
1345 representing two models of the landscape evolution in the Bay of Roscanvel following the sea  
1346 level rise (b). On each model, the typical foraminifera encountered in the different  
1347 environments according to their ecology were added.

1348 Figure 12: a) Published reconstituted palaeoclimatic data across the Holocene in the North  
1349 Atlantic region (solar irradiance (dTSi) by *Steinhilber et al. 2009*, Sea surface temperature  
1350 (SST) by *Jiang et al., 2015* and Northern Hemisphere summer insolation by *Berger and*  
1351 *Loutre, 1991*) and the detrital Hematite Stained Grains by *Bond et al., 2008*. b) Diagram  
1352 showing the palynological data of the “A” core between 6,600 and 5,400 years Cal. BP. (from  
1353 left to right: pollen and dinocyst concentrations, tree percentages, *Corylus*, *Alnus*, percentages  
1354 and the *L. machaerophorum* / *S. bentorii* ratio). c) Diagram showing the palynological data of  
1355 the VC-08 core between 8,700 and 8,400 years Cal. BP with the same succession of  
1356 palynological proxies. The temporal extent of each core is represented by a black rectangle in  
1357 the a) part and the temporal extent of the graphs b) and c) is represented by a blue rectangle.  
1358 The limits of palynozones A-B / A-C and VC-B / VC-C have also been reported in the a) part  
1359 of the figure.

1360 Figure 13: Pollen grains photographs of wild Poaceae (a) and cereals (b), with grain and  
1361 *annulus* diameter measurements for each one, on 4 levels of the VC-08 core.

1362 Figure 14: Diagram in depth from the VC-08 core, representing variations of some  
1363 herbaceous taxa percentages (i.e. *Cerealina*-type, other Poaceae, *Brassicaceae*, *Rumex* sp.) and  
1364 the occurrences of *Plantago lanceolata*.

1365 Figure 15: Map showing the first occurrences of *Cerealia* in published pollen records, with  
1366 related dates. The two circled areas (Teviecien and Retzien) delimit the cultural specificities  
1367 of the end of the Mesolithic after *Marchand (2005)*. The gray arrows correspond to the  
1368 different neolithisation paths reaching Western Europe.

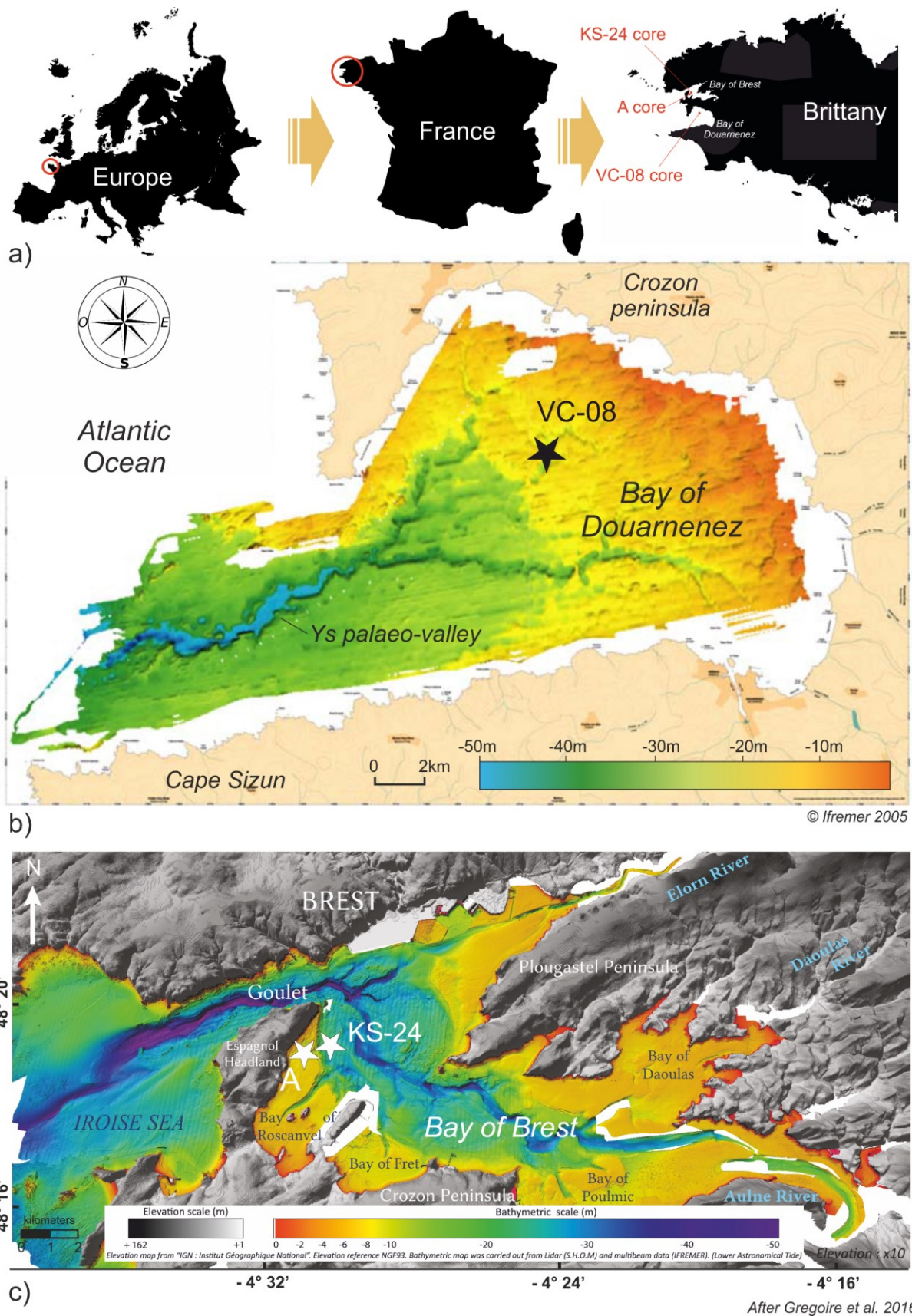


Figure 1

Schematic scenario of Bay of Douarnenez sedimentary infilling  
(after Le Roy and Jouet, 2005)

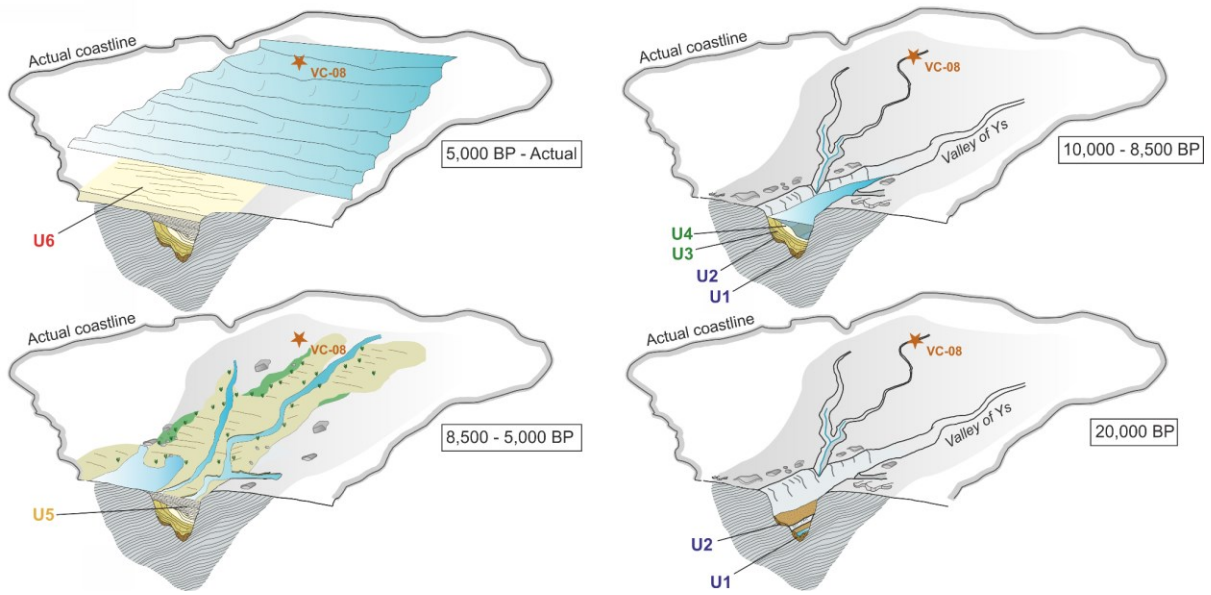


Figure 2

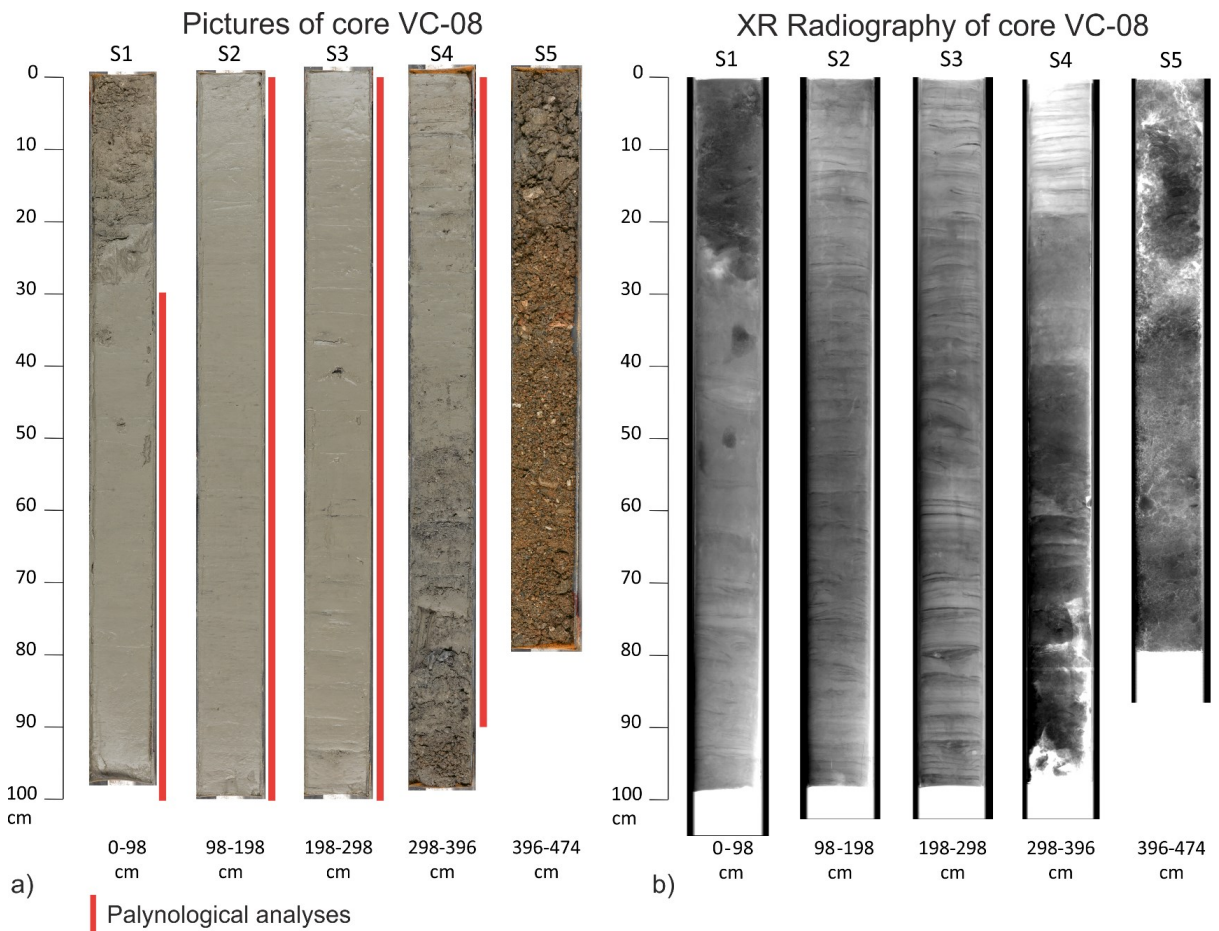


Figure 3

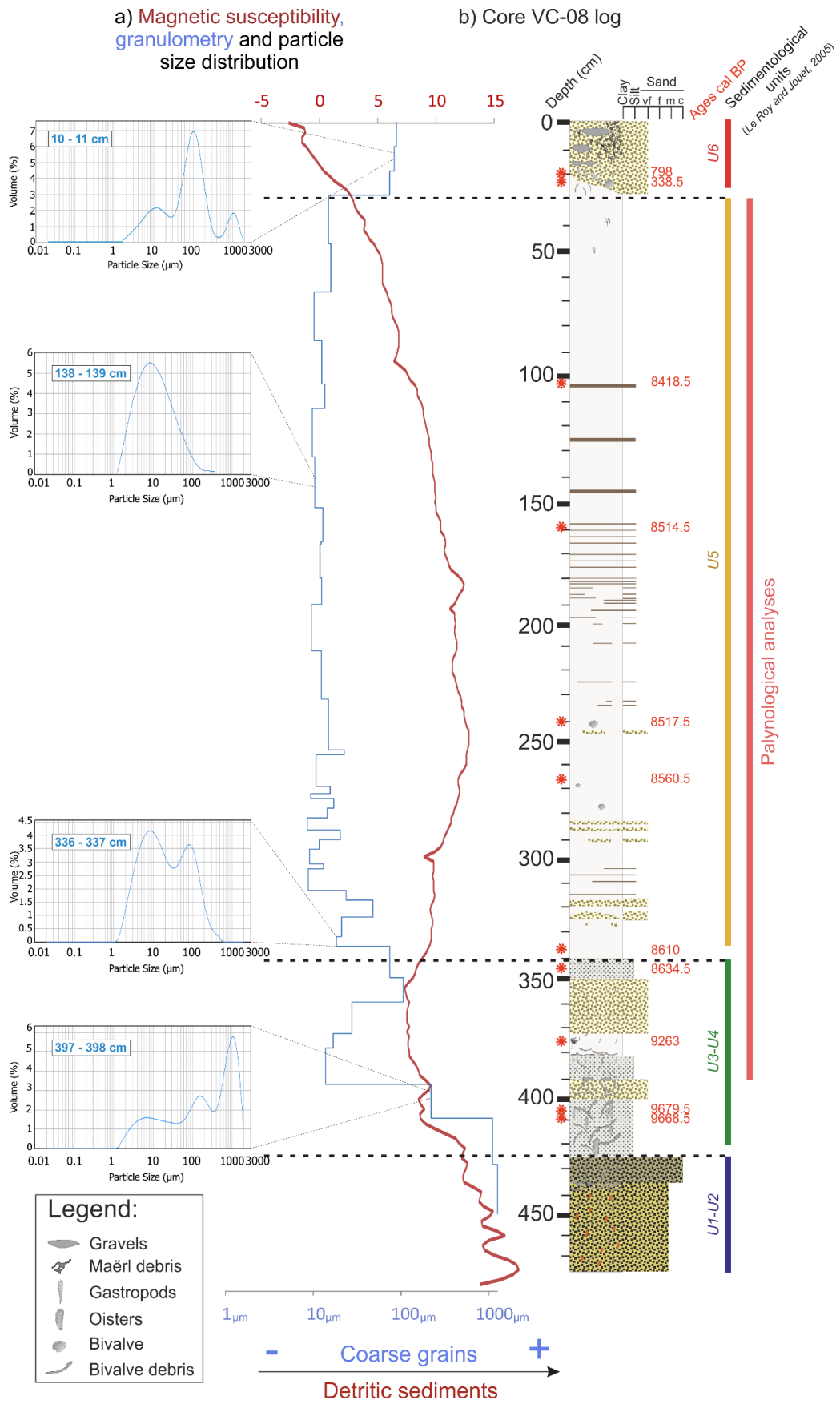


Figure 4



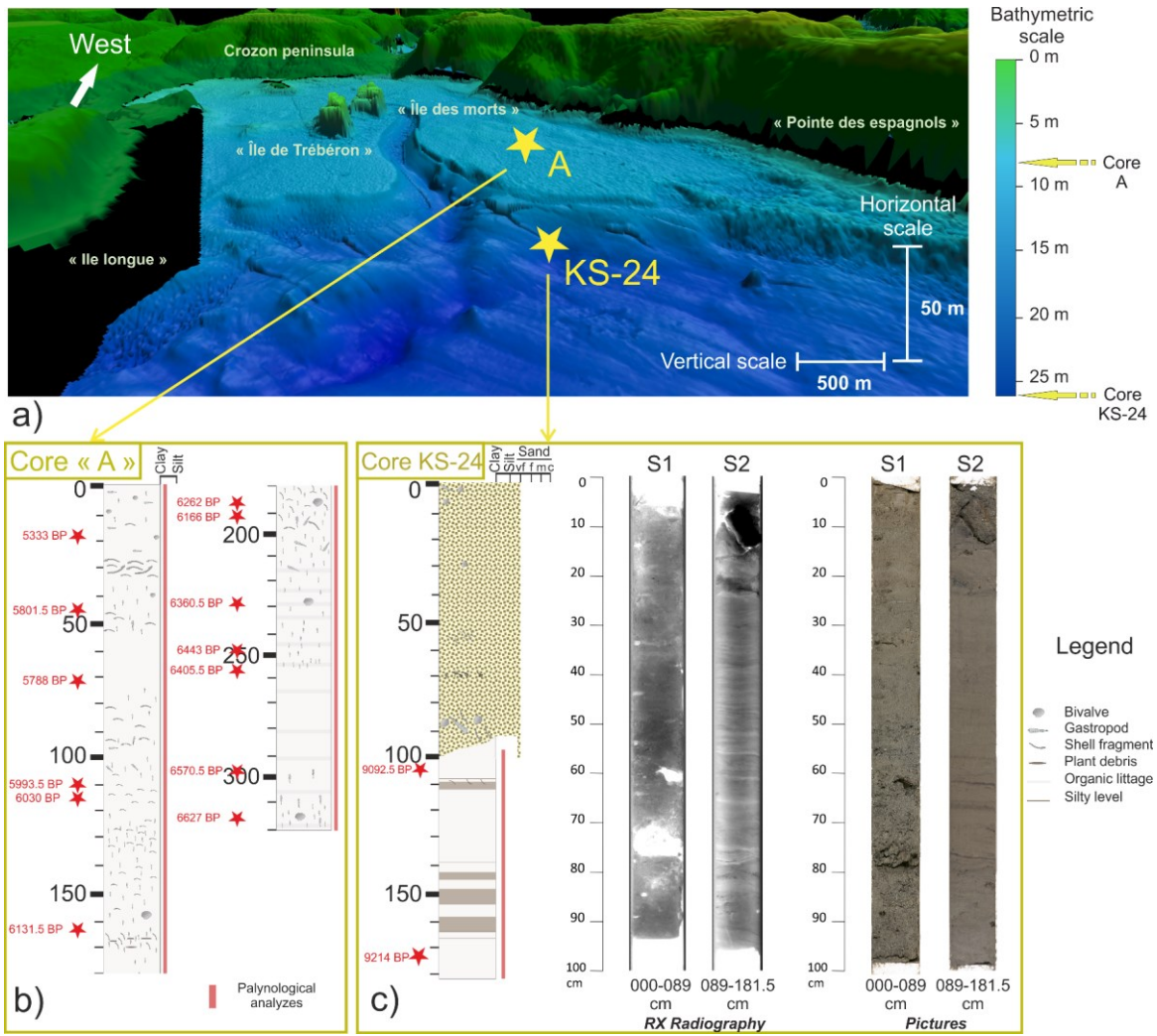


Figure 5

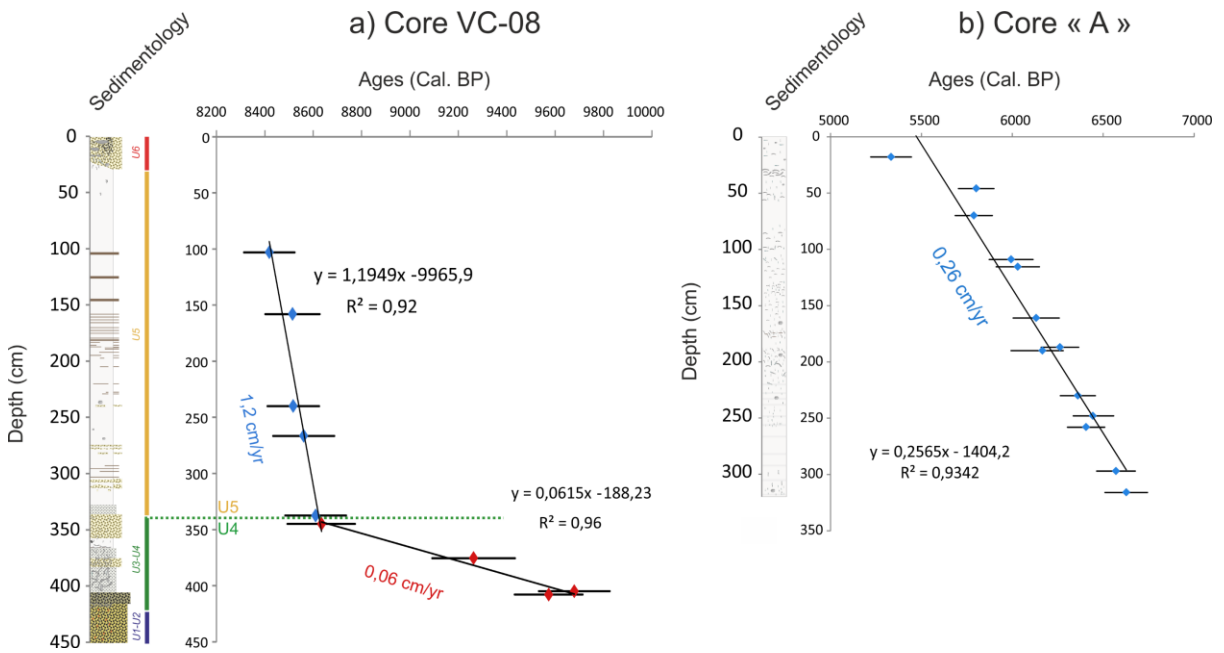


Figure 6

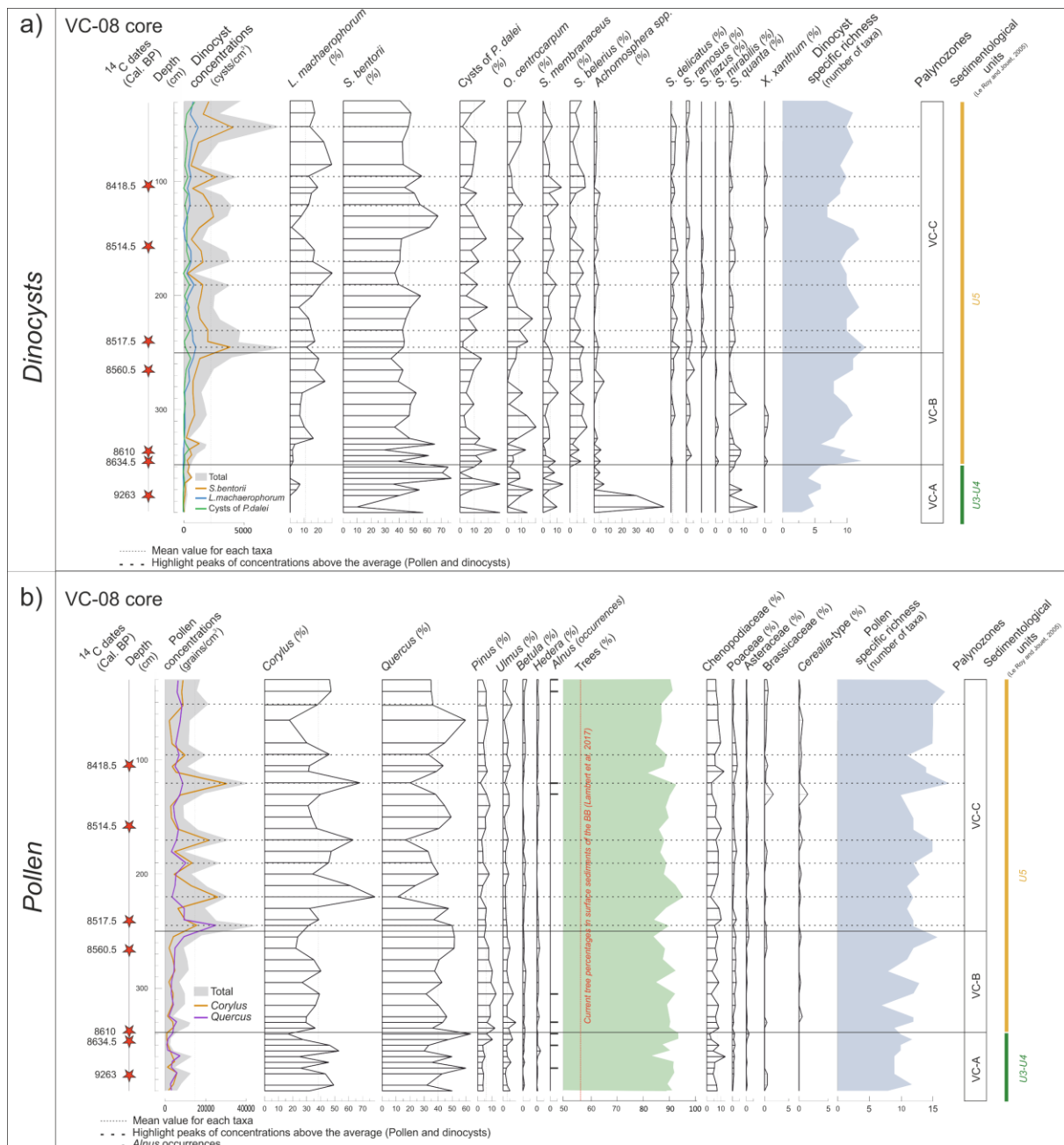


Figure 7

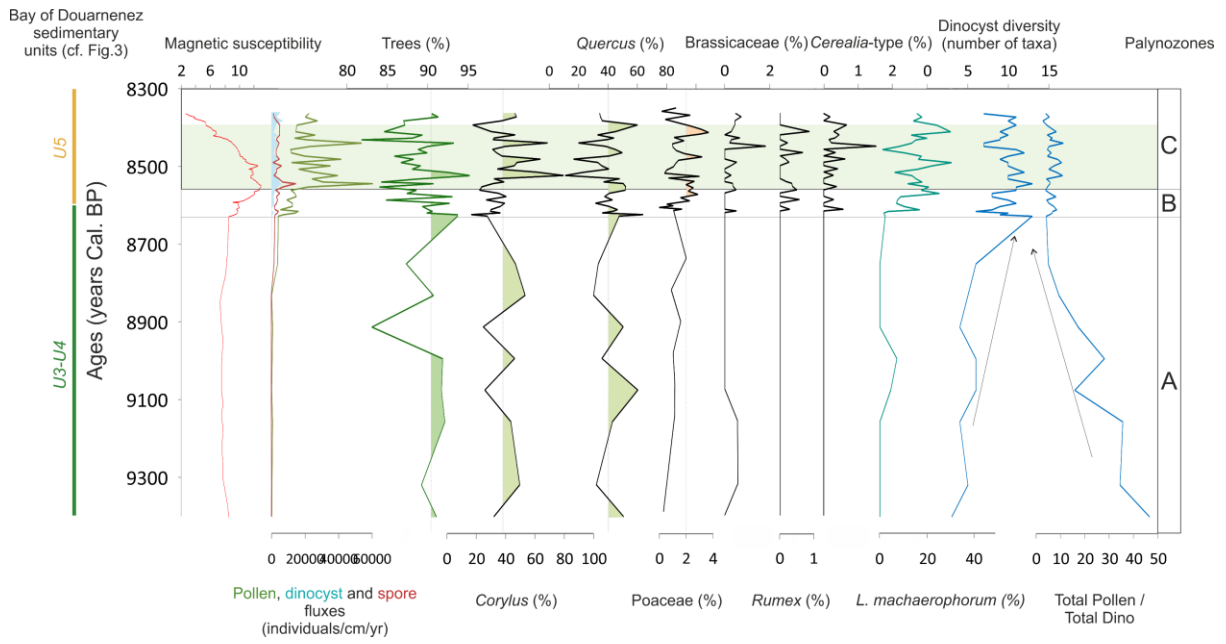


Figure 8

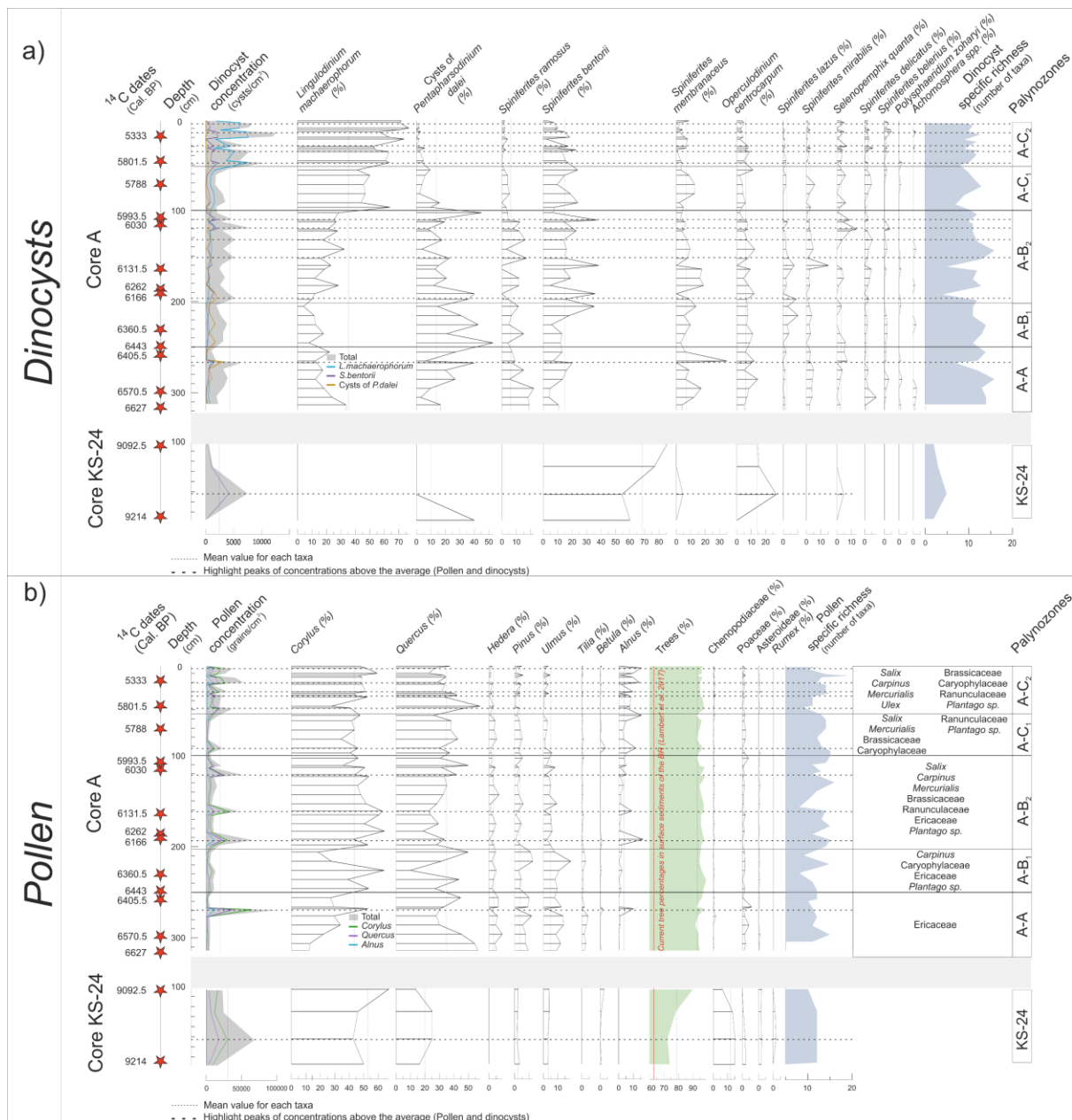


Figure 9

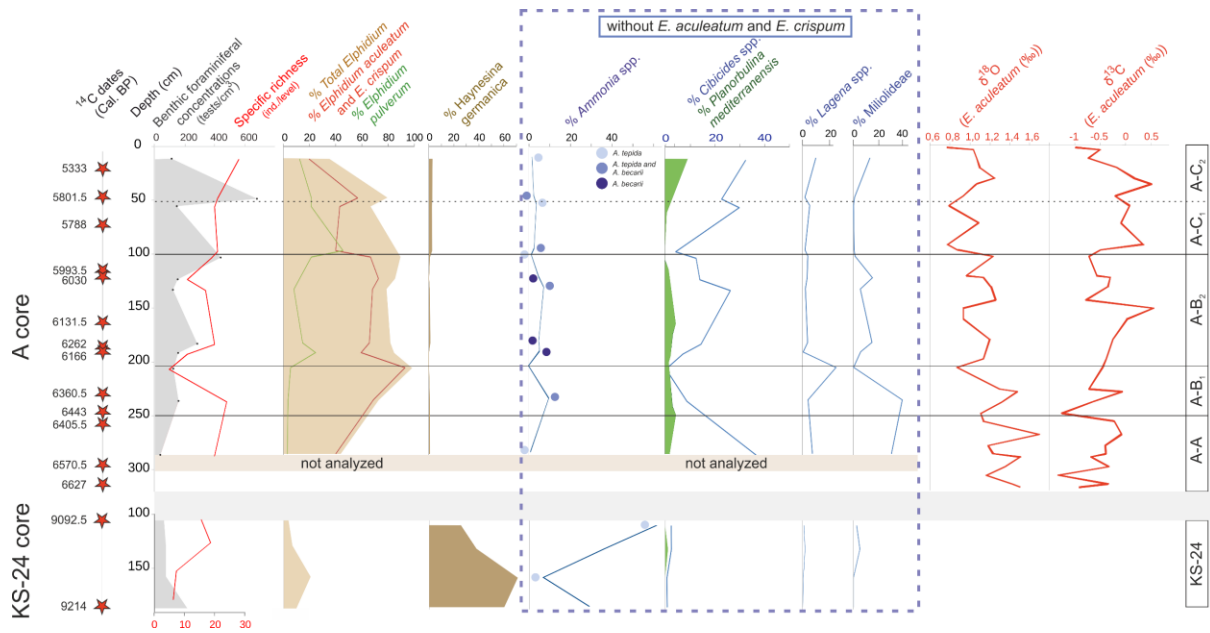


Figure 10

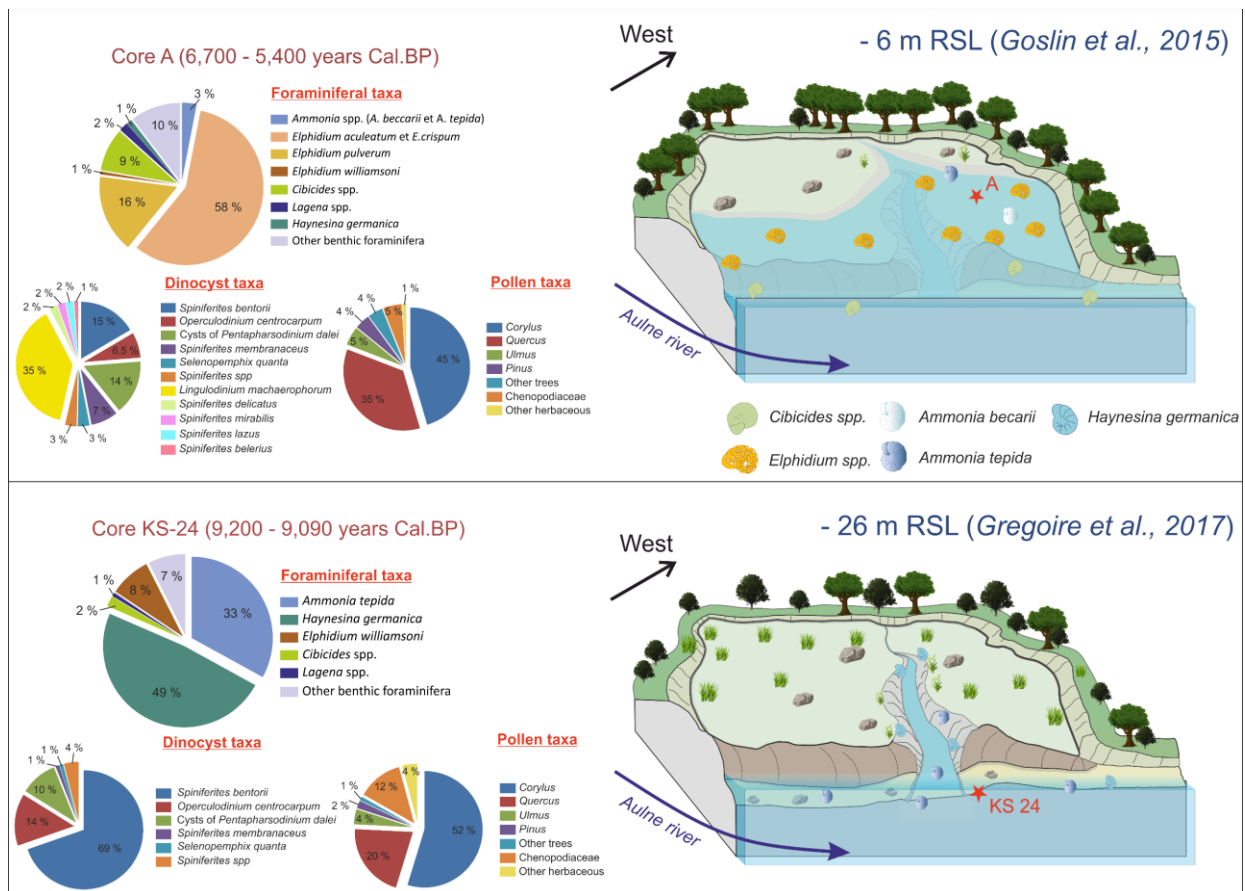


Figure 11

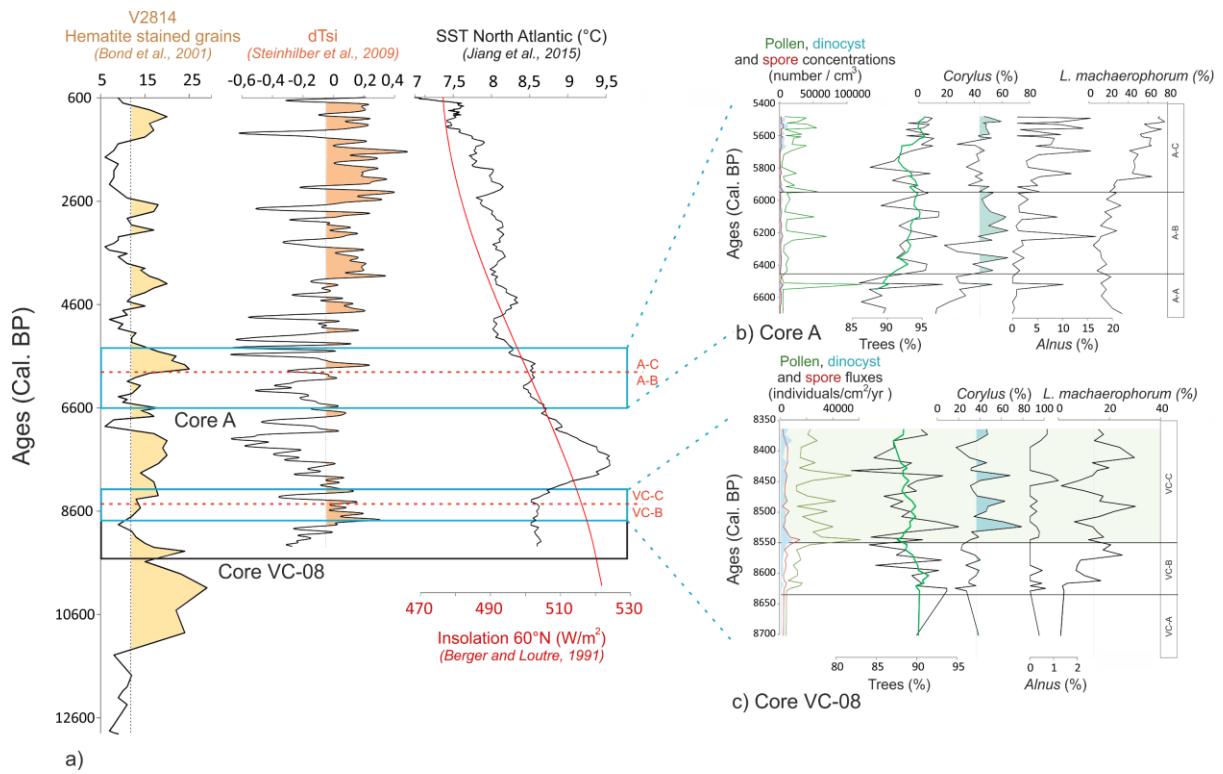


Figure 12

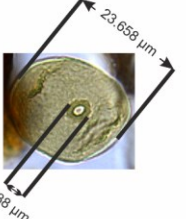
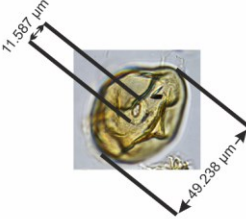
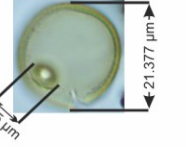
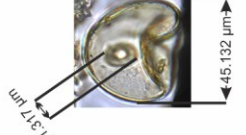
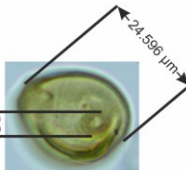
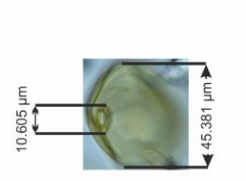
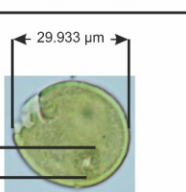
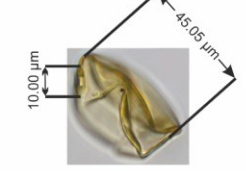
Core VC-08	a) Poaceae	b) Cerealia-type
120 cm 8441 years BP		
140 cm 8457 years BP		
220 cm 8524 years BP		
325 cm 8612 years BP		

Figure 13

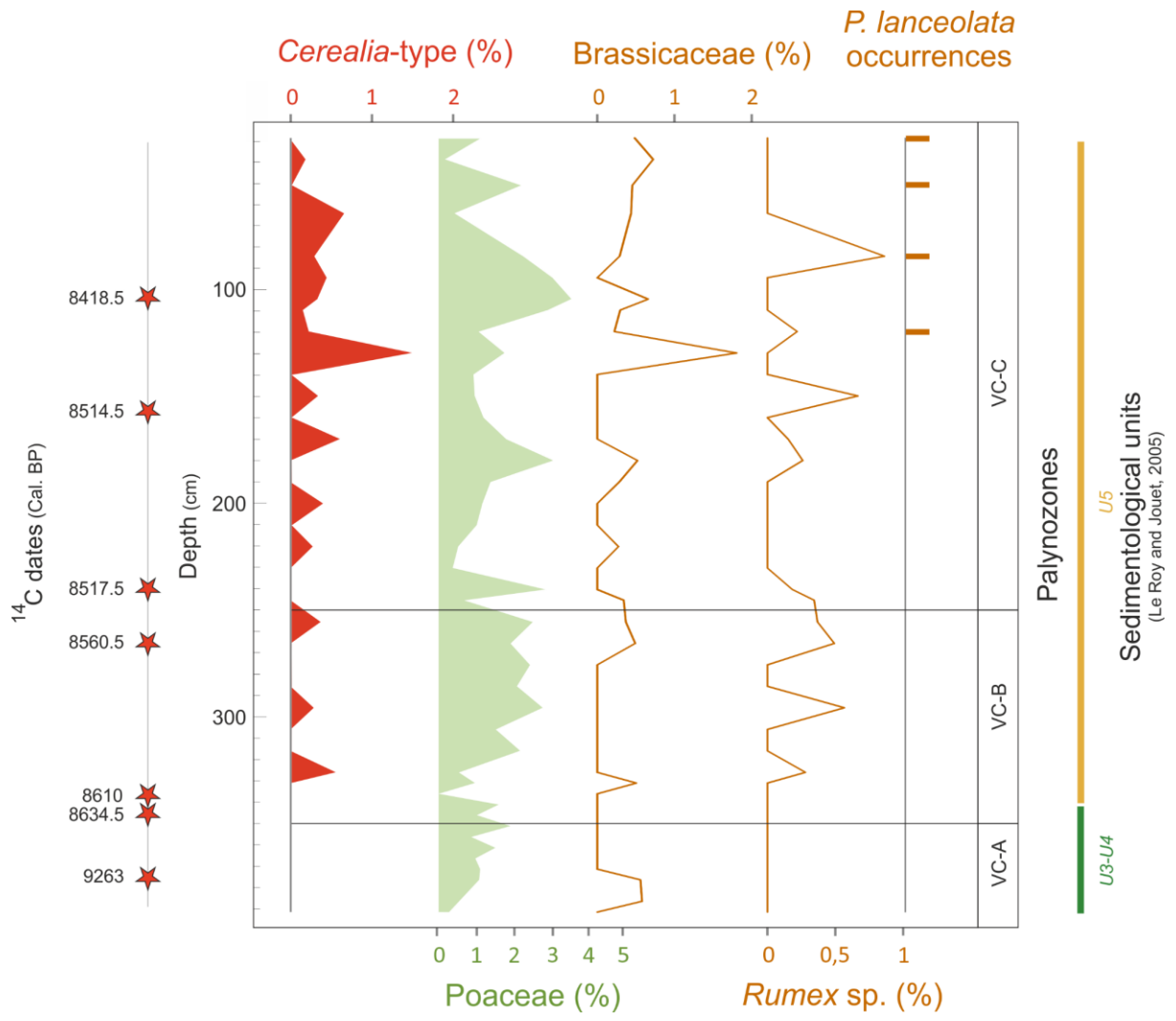


Figure 14



1. Cupillard et al., 1994 ; 2. Nielsen, 2003 ; 3. Lotter, 1999 and Tinner et al., 2007 ; 4. Beckmann, 2004 ;  
 5. Erny-Rodmann et al., 1997 ; 6. Tinner et al., 1999 ; 7, 8. Triat-Laval, 1978 ; 9. Puertas, 1999 ; 10. Guenet, 1995 ;  
 11. Jalut and Vernet, 1989 ; 12. Amat, 1995 ; 13. Galop and Vaquer, 2004 ; 14. Legigan and Marambat, 1993 ;  
 15. Joly and Visset, 2005 ; 16. Joly and Visset, 2009 ; 17. Visset et al., 1996 ; 18. Ouguerram and Visset, 2001 ;  
 19. Visset et al., 2001 ; 20. Carcaud et al., 2000 ; 21, 22. Leroyer and Allenet, 2006 ; 23, 24. Ruffaldi, 1999 ;  
 25. This study

Figure 15